NISTIR 4768

Finite-Rate Diffusion-Controlled Reaction in a Vortex A Report

Ronald R. Rehm*
Howard R. Baum**
Hai C. Tang*
Daniel W. Lozier*

U.S. DEPARTMENT OF COMMERCE
Technology Administration
National Institute of Standards
and Technology
Computing and Applied Mathematics Laboratory*
Building and Fire Research Laboratory**
Gaithersburg, MD 20899

U.S. DEPARTMENT OF COMMERCE
Rockwell A. Schnabel, Acting Secretary

NATIONAL INSTITUTE OF STANDARDS AND TECHNOLOGY
John W. Lyons, Director

NISTIR 4768

Finite-Rate Diffusion-Controlled Reaction in a Vortex A Report

Ronald R. Rehm*
Howard R. Baum**
Hai C. Tang*
Daniel W. Lozier*

U.S. DEPARTMENT OF COMMERCE
Technology Administration
National Institute of Standards
and Technology
Computing and Applied Mathematics Laboratory*
Building and Fire Research Laboratory**
Gaithersburg, MD 20899

February 1992

U.S. DEPARTMENT OF COMMERCE
Rockwell A. Schnabel, Acting Secretary

NATIONAL INSTITUTE OF STANDARDS AND TECHNOLOGY
John W. Lyons, Director

Finite-Rate Diffusion-Controlled Reaction in a Vortex A Report

Ronald G. Rehm,* Howard R. Baum†, Hai C. Tang‡
and Daniel W. Lozier §
National Institute of Standards and Technology
Gaithersburg, MD 20899

February 10, 1992

Abstract

A two-dimensional model of a constant-density diffusion-controlled reaction with finite reaction-rate chemistry occurring between unmixed species initially occupying adjacent half-spaces is formulated and analyzed. The chemical reaction term is taken to be appropriate for an isothermal, bimolecular reaction for simplicity. An axisymmetric viscous vortex field satisfying the Navier-Stokes equations winds up the interface between the species as they diffuse together and react. The diffusion rates for the two species are assumed constant and equal so that a mixture fraction or Shvab-Zeldovich variable can be used. The resulting equation for the mixture fraction is linear and can be solved by noting that a Lagrangian coordinate system removes the convection and that the equation permits a global similarity solution. The single nonlinear equation for one species is also analyzed in a Lagrangian coordinate system. The dimensionless equations depend upon three parameters, Reynolds number, Schmidt number and the initial species concentration ratio, while the dimensionless time plays the role of a Damköhler number. For large Schmidt numbers, a simple expression for the mixture fraction can be obtained and the nonlinear equation for the species concentration can also be substantially simplified. Asymptotic and numerical results show the structure of the reaction region and the competing influences of reaction, diffusion and convection.

1 Introduction

Investigation of turbulent combustion has become an area of greatly increased activity over the past several years. This activity has occurred because both theoretical and experimental

*Computing and Applied Mathematics Laboratory
†Building and Fire Research Laboratory
‡Computing and Applied Mathematics Laboratory
§Computing and Applied Mathematics Laboratory

progress has been made in the understanding of the governing processes and because of the great technological importance of turbulent combustion. In earlier papers [4], [8], we have mentioned some of the progress and discussed models which we have developed to examine turbulent combustion processes. In particular, experiments indicate that, when the Reynolds number is large, the length and time scales associated with turbulent combustion in fires can be separated and analyzed individually. At the largest length scales, the geometry defines the flow field, which is essentially inviscid or nondissipative away from boundaries. At smaller scales, where the combustion occurs, diffusion of the fuel and oxidizer into each other and reaction takes place, with subsequent reactant consumption and heat release. Finally, at still smaller scales, the structure of the reaction zone in individual flamelets is important and chemical species concentrations can be determined. The essence of the model of fire-induced turbulent combustion outlined in [4] is to analyze each of these three scales separately at first, and then to couple them through their dynamical interactions subsequently.

Marble [3] proposed a two dimensional model problem of small-scale mixing and reaction, which he and his students studied extensively through analytical means [5], [6] and [7]. The model is important because it includes the two-dimensional effects of flame stretching and convective enhancement of diffusion in a diffusion-controlled reaction in a viscously spreading vortex. The analytical method utilized by Marble and students to attack this problem is based on a technique developed earlier by Carrier, Fendell and Marble [1] in which the flame front is analyzed locally, assuming that the front is sharp, and summing over this flame front to obtain global dependences of consumption rates upon the governing parameters. While important scaling results are obtained, the mathematical limitations of the analyses are not clear from the presentations [3], [5], [6] and [7], a fact pointed out by Rehm et al [8] and addressed in their analysis.

In the present paper, the authors extend the analysis presented in [8] to consider the effects of finite-rate chemistry. In Section 2 we formulate the problem and give its mathematical description when there is a time scale associated with the combustion chemistry. In Section 3 the case of infinite-rate chemistry is reconsidered and an asymptotic solution for large Schmidt number (small species diffusion) is presented. This solution is new and much simpler than that previously presented [8]. Transformations of the independent variables make analysis of the problem more tractable. In Section 4 this analysis is applied to the case of constant-temperature finite-rate chemistry and the results of the analysis are compared with the infinite-rate case. The dependence upon governing parameters of the fuel consumption rate (and therefore the heat release rate) is examined. In Section 5, numerical results are presented.

2 Formulation of the Problem

Consider the model in which initially there is fuel in the left half-plane and oxidizer in the right half-plane in arbitrary proportions. These half-spaces are brought into contact and simultaneously a line vortex with axis at the origin is imposed (see Figure 1). The vortex induces a convective mixing of the interface between the two species, increasing the area of the separating surface in the neighborhood of the origin and enhancing the diffusion of the species into each other. It is assumed that the reaction rate does not depend upon temperature, i.e.,

that the reaction remains isothermal, and that the reaction is bimolecular. The chemical reaction is assumed to take place at constant density and all diffusion coefficients (kinematic viscosity, thermal and concentration coefficients) are assumed to be constant. The tangential velocity v_θ imposed is

$$v_\theta(r,t) = r\frac{d\theta}{dt} = \frac{\Gamma}{2\pi r}[1-\exp(-\eta)] \tag{1}$$

where Γ is the circulation of the vortex, ν is the kinematic viscosity and $\eta = r^2/4\nu t$ is a similarity variable.

With the assumptions described above, the species equations are decoupled from the momentum and continuity equations; they are equations representing a balance between convection, diffusion and reaction.

$$\frac{\partial Y_i}{\partial t} + \frac{v_\theta}{r}\frac{\partial Y_i}{\partial \theta} - D\left(\frac{\partial^2 Y_i}{\partial r^2} + \frac{1}{r}\frac{\partial Y_i}{\partial r} + \frac{1}{r^2}\frac{\partial^2 Y_i}{\partial \theta^2}\right) = -\tilde{k}Y_1Y_2 \tag{2}$$

where $i = 1,2$ and D are the species diffusion coefficients, assumed to be constant and equal. Here Y_i is the mass-fraction of species i and is dimensionless. The initial conditions are that $Y_1 = Y_{10}, Y_2 = 0$ for $\pi/2 \le \theta \le 3\pi/2$ and $Y_1 = 0, Y_2 = Y_{20}$ for $-\pi/2 \le \theta \le \pi/2$.

Rather than solve directly Eqs.(2), we will introduce other dependent variables, the mixture-fraction variable and the difference between one species concentration and the mixture-fraction variable. Define the mixture fraction variable

$$Z = \frac{Y_1 - Y_2 + Y_{20}}{Y_{10} + Y_{20}} \tag{3}$$

Note that a linear combination of equations (2) eliminates the nonlinear reaction term and yields a linear equation for the mixture fraction.

$$\frac{\partial Z}{\partial t} + \frac{v_\theta}{r}\frac{\partial Z}{\partial \theta} - D\left(\frac{\partial^2 Z}{\partial r^2} + \frac{1}{r}\frac{\partial Z}{\partial r} + \frac{1}{r^2}\frac{\partial^2 Z}{\partial \theta^2}\right) = 0 \tag{4}$$

with initial conditions $Z = 1$ for $\pi/2 \le \theta \le 3\pi/2$ and $Z = 0$ for $-\pi/2 \le \theta \le \pi/2$. This equation determines the solution to the infinite-rate or flame-sheet problem and was solved in [8].

Using the mixture fraction variable Z, eliminate one of the species in Eqs. (2)

$$Y_2 = Y_1 + Y_{20} - (Y_{10} + Y_{20})Z \tag{5}$$

Then the equation for the Y_1 has the same left side as before while the right side is $-\tilde{k}Y_1[Y_1 + Y_{20} - (Y_{10} + Y_{20})Z]$. We then change the dependent variable from Y_1 to W.

$$W(\rho,\theta_0,\tau) = Y_1(\rho,\theta_0,\tau)/Y_{10} - Z(\eta,\theta_0) \tag{6}$$

This change of variables eliminates any difficulty arising from the discontinuous initial conditions in the species concentrations. The equation for W is

$$\frac{\partial W}{\partial t} + \frac{v_\theta}{r}\frac{\partial W}{\partial \theta} - D\left(\frac{\partial^2 W}{\partial r^2} + \frac{1}{r}\frac{\partial W}{\partial r} + \frac{1}{r^2}\frac{\partial^2 W}{\partial \theta^2}\right) = -\tilde{k}(W+Z)[Y_{10}W + Y_{20}(1-Z)] \tag{7}$$

The initial conditions are that $W = 0$ at $t = 0$ and the boundary conditions are that $W \to 0$ as $r\cos\theta \to \pm\infty$ away from $\theta = \pm\pi/2$.

The problem is made dimensionless using the kinetics time scale $\tau_0 = 1/\tilde{k}Y_{20}$, the length scale defined by this time and the diffusion coefficient $l = \sqrt{D/\tilde{k}Y_{20}}$ and the concentrations with respect to their initial values. With this scaling, the dimensionless time becomes a Damköhler number. Three dimensionless parameters enter the problem, the ratio of initial concentrations, $\alpha \equiv Y_{10}/Y_{20}$, the Schmidt number, $\mathrm{Sc} \equiv \nu/D$, and the Reynolds number, $\mathrm{Re} \equiv \Gamma/(4\pi\nu)$. First, the similarity variable becomes

$$\eta = r^2/(4\,\mathrm{Sc}\,t) \tag{8}$$

while equations (1) and (5) become

$$v_\theta(r,t) = rd\theta/dt = 2\,\mathrm{Re}\,\mathrm{Sc}\,/r[1-\exp(-\eta)] \tag{9}$$

$$Y_2/Y_{20} = \alpha W + 1 - Z \tag{10}$$

Finally, the Eqs. (2), (4) and (7) for the dependent variables become

$$\frac{\partial Y_i}{\partial t} + \frac{v_\theta}{r}\frac{\partial Y_i}{\partial \theta} - \left(\frac{\partial^2 Y_i}{\partial r^2} + \frac{1}{r}\frac{\partial Y_i}{\partial r} + \frac{1}{r^2}\frac{\partial^2 Y_i}{\partial \theta^2}\right) = -Y_1 Y_2 \tag{11}$$

$$\frac{\partial Z}{\partial t} + \frac{v_\theta}{r}\frac{\partial Z}{\partial \theta} - \left(\frac{\partial^2 Z}{\partial r^2} + \frac{1}{r}\frac{\partial Z}{\partial r} + \frac{1}{r^2}\frac{\partial^2 Z}{\partial \theta^2}\right) = 0 \tag{12}$$

$$\frac{\partial W}{\partial t} + \frac{v_\theta}{r}\frac{\partial W}{\partial \theta} - \left(\frac{\partial^2 W}{\partial r^2} + \frac{1}{r}\frac{\partial W}{\partial r} + \frac{1}{r^2}\frac{\partial^2 W}{\partial \theta^2}\right) = -(W+Z)(\alpha W + 1 - Z) \tag{13}$$

where all variables are dimensionless.

As in [8] we change to Lagrangian coordinates. Integrating the tangential velocity gives the angle $\theta(r,\theta_0,t)$ at time t for any fluid element initially located at r,θ_0 . A change of variables to the Lagrangian coordinates, ρ,θ_0,τ,

$$\begin{aligned} r &= \rho \\ \theta &= \theta_0 + \frac{\mathrm{Re}}{2}\frac{1-E_2(\eta)}{\eta} \\ t &= \tau \end{aligned} \tag{14}$$

where $E_j(z) = \int_1^\infty t^{-j}\exp(-zt)dt$, can then be made in the all of the equations. For the problem posed above for the mixture-fraction variable, which is the flame-sheet model (and which we call the Marble problem [3]), there are no length or time scales, and we find that Z is only a function of the similarity variable η and the angle θ_0.

In [8] the Marble problem was solved by Fourier analyzing the mixture fraction variable in the Lagrangian angle θ_0, solving the linear, two-point boundary value problem by asymptotic

and numerical methods, and Fourier synthesizing the complete solution. The asymptotic analysis involved a large-Schmidt-number approximation, and the simplification resulting from that approximation was noted. This simplification allows the results to be interpretated physically in a much more straight-forward fashion. The applicablity of this approximation was tested against the direct numerical solution of the equations, and the conclusion was that the large-Schmidt-number approximation has wider applicability than one might initially expect. Recent experimental evidence [9] comparing mixing in liquids and gases comfirms the conclusion that a large-Schmidt-number approximation, which is definitely valid in liquids, is qualitatively (and approximately quantitatively) valid also in gases. In the next section a new, much simpler asymptotic solution is derived for the mixture fraction when the Schmidt number is large. The asymptotic results compare well with those obtained in [8] over ranges of interest. The method used to obtain the mixture fraction is then utilized in the following section on the more general problem with finite rate kinetics.

3 Flame-Sheet Problem

In this section, we concentrate on Eq. (12), the Marble problem, and obtain a quite simple asymptotic solution valid for large Schmidt numbers. This solution is new and simplifies considerably the solution of the more general problem where one is interested in the effects of finite-rate chemistry. The use of Lagrangian coordinates eliminates the need to resolve small-scale internal transition layers which arise when the Reynolds number is large. With this transformation the problem reduces simply to a time-dependent diffusion problem. The equation for the mixture fraction in Lagrangian variables becomes:

$$\frac{\partial Z}{\partial \tau} - \left(\frac{\partial^2 Z}{\partial \rho^2} + \frac{1}{\rho}\frac{\partial Z}{\partial \rho} + \left[\left(\mathrm{Re}\,\frac{1-e^{-\eta}}{\eta} \right)^2 + 1 \right] \frac{1}{\rho^2}\frac{\partial^2 Z}{\partial \theta_0^2} \right)$$
$$- \left(\frac{2\,\mathrm{Re}}{\rho^2} \left(e^{-\eta} - \frac{1-e^{-\eta}}{\eta} \right) \frac{\partial Z}{\partial \theta_0} + \frac{\mathrm{Re}}{\rho}\frac{1-e^{-\eta}}{\eta}\frac{\partial^2 Z}{\partial \rho \partial \theta_0} \right) = 0 \qquad (15)$$

The solution depends upon the similarity variable and angle.

It is more convenient to use the similarity variable, $\eta = \rho^2/(4\,\mathrm{Sc}\,\tau)$, and the Lagrangian coordinate normal to the interface between the fuel and the oxidizer, $\zeta = \sqrt{Sc\eta}cos\theta_0$. The resulting equation for the mixture fraction is messy and is not stated here. However, this equation simplifies considerably and allows additional analysis when the Schmidt number is large. For large Schmidt numbers and for $\eta > 0$, Eq. (15) becomes

$$\eta\frac{\partial Z}{\partial \eta} + \frac{\zeta}{2}\frac{\partial Z}{\partial \zeta} + \frac{1}{4}\left[\left(\mathrm{Re}\,\frac{1-e^{-\eta}}{\eta} \right)^2 + 1 \right] \frac{\partial^2 Z}{\partial \zeta^2} = 0 \qquad (16)$$

where $Z \to 1$ as $\zeta \to -\infty$ and $Z \to 0$ as $\zeta \to \infty$.

We now make a final change in variables from ζ to μ

$$\mu = \zeta f(\eta) \qquad (17)$$

where

$$f(\eta) = \frac{1}{\sqrt{1 + \mathrm{Re}^2 f_1(\eta)}}$$
$$f_1(\eta) = [1/3 - 2E_4(\eta) + E_4(2\eta)]/\eta^2 \tag{18}$$
$$E_j(x) = \int_1^\infty t^{-j} \exp(-xt)dt$$

Function $f_1(\eta)$ was introduced in [8], where its properties were discussed.

With this new independent variable, and assuming that Z only depends on μ, Eq.(16) becomes

$$2\mu \frac{\partial Z}{\partial \mu} + \frac{\partial^2 Z}{\partial \mu^2} = 0 \tag{19}$$

and this equation has solution

$$Z(\mu) = (1/2)\,\mathrm{erfc}\,(\mu) \tag{20}$$

satisfying boundary conditions that $Z \to 1$ as $\mu \to -\infty$ and $Z \to 0$ as $\mu \to \infty$. This corresponds to boundary conditions in Eq. (16) stated in terms of η and ζ. It should be noted that the error function profile for Z, which also emerges in the approximate analyses noted above, is here derived in terms of the asymptotically exact independent variable.

4 Finite-Rate Chemistry Problem

Changing variables from Eulerian to Lagrangian in Eq.(13) yields the corresponding equation for W

$$\frac{\partial W}{\partial \tau} - \left(\frac{\partial^2 W}{\partial \rho^2} + \frac{1}{\rho}\frac{\partial W}{\partial \rho} + \left(\left(\mathrm{Re}\,\frac{1-e^{-\eta}}{\eta}\right)^2 + 1\right)\frac{1}{\rho^2}\frac{\partial^2 W}{\partial \theta_0^2}\right)$$
$$- \left[\frac{2\,\mathrm{Re}}{\rho^2}\left(e^{-\eta} - \frac{1-e^{-\eta}}{\eta}\right)\frac{\partial W}{\partial \theta_0} + \frac{2\,\mathrm{Re}}{\rho}\frac{1-e^{-\eta}}{\eta}\frac{\partial^2 W}{\partial \rho \partial \theta_0}\right] \tag{21}$$
$$= -[W + Z][\alpha W + 1 - Z]$$

with initial conditions that $W = 0$ at $\tau = 0$ and boundary conditions that $W \to 0$ as $\rho\cos(\theta_0) \to \pm\infty$ for θ_0 away from $\pm\pi/2$.

For large Schmidt number (to lead order in Sc), the equation for the dimensionless species concentration becomes, for $\eta > 0$,

$$t\frac{\partial W}{\partial t} - \eta\frac{\partial W}{\partial \eta} - \frac{\zeta}{2}\frac{\partial W}{\partial \zeta} - \frac{1}{4}\left[\left(\mathrm{Re}\,\frac{1-e^{-\eta}}{\eta}\right)^2 + 1\right]\frac{\partial^2 W}{\partial \zeta^2} \tag{22}$$
$$= -t(W + Z)(\alpha W + 1 - Z)$$

where the boundary conditions are that $W \to 0$ as $\zeta \to \pm\infty$.

With a change of variables to $\mu, \acute{\eta} = \eta/t$ and $\acute{t} = t$, Eq.(22) becomes

$$\acute{t}\frac{\partial W}{\partial \acute{t}} - \frac{1}{4}F(\acute{\eta}/\acute{t})(2\mu\frac{\partial W}{\partial \mu} + \frac{\partial^2 W}{\partial \mu^2}) = -\acute{t}[W + Z(\mu)][\alpha W + 1 - Z(\mu)] \tag{23}$$

where

$$F(\eta) = \left[\left(\mathrm{Re} \frac{1 - \exp(-\eta)}{\eta} \right)^2 + 1 \right] f^2(\eta) \tag{24}$$

and where $W \rightarrow 0$ as $\mu \rightarrow \pm\infty$.

We now discuss some of the properties of Eq.(23). Note again that, in the dimensionless variables used, the time is a Damköhler number, i.e., the ratio of a residence time for diffusion to the chemical reaction time. First, away from the reaction zone (i.e., for $\acute{\eta}$ and μ not too small and for $\acute{t}$ not too large), the right side must be zero. Setting this term, the chemical reaction term, to zero implies either that $W + Z(\mu)$ or $\alpha W + 1 - Z(\mu)$ is zero. If the first term is zero, both W and Z are zero, and therefore, we are in the region where there is all fuel (and no reaction). Similarly, if the second term is zero, both W and $1 - Z$ are zero, and we are in the region where there is all oxidizer (and no reaction). Also, for large η' or small t', and any μ, the equation reduces to that of the one-dimensional (1-D) version the problem (the diffusion-reaction problem with no vortex field).

We have formulated this 1-D problem as two coupled equations, one for the mixture fraction and the second for the dimensionless species concentration, and we have utilized the fact that a similarity solution exists for the case of infinite-rate chemistry. When the 1-D problem is formulated in this fashion, Eq.(23) is obtained with $F(\eta) \equiv 1$, $\mu = \zeta = x/(2\sqrt{\mathrm{Sc}\, t})$ and x, t the dimensionless distance and time, with $\mathrm{Sc} \equiv 1$. The important point to note is that the two-dimensional problem reduces to the one-dimensional case when either the Reynolds number is zero (i.e., the circulation of the imposed vortex is set to zero) or at large distances from the vortex center where the imposed velocity vanishes. We note that the equation above for the dimensionless species concentration in the large-Schmidt-number approximation generally is close to the one-dimensional equation when the function $F(\eta'/t')$ is approximately unity, and this occurs, as seen in Eq.(24), when either the Reynolds number is small or at large distances relative to the diffusion of vorticity at a specified time (large η). In the first subsection below, we will also find that the 1-D equation is a good approximation to the full 2-D problem even for large Re provided that the time is small and radius not too small.

This one-dimensional problem has been formulated earlier and solved by asymptotic methods by Kapila [2] in a manner somewhat different than that described above. Specifically, Kapila formulated the problem as two coupled equations for the dimensionless species concentrations. He noted specifically, that his formulation does not require that the diffusivities be equal (and therefore has an additional parameter representing the ratio of diffusivities for the two species). He determined asymptotically the properties of this 1-D reaction-diffusion problem both at early and late dimensionless times. Specifically, he determined the structure of the flame sheet as time becomes large relative to the chemical kinetics time scale.

The one-dimensional problem solved by Kapila [2] can be used to deduce much of the structure of the solution to the present problem. The solution for the 1-D reaction-diffusion problem determines completely the reaction-diffusion structure in the far field (away from the imposed vortex) since Eq.(23) is the generalized problem with a variable diffusion coefficient $F(\eta)$ which depends only upon the parameter η. The asymptotic analyses presented by Kapila reveal the structure of the reaction-diffusion zone in regions away from the influence

of the vortex. In particular, for small times (or Damköhler number), the reaction has not been able to progress far. Each species is initially a step function with all fuel to the left of the interface and all oxidizer to the right. At early times, each diffuses according to the 1-D solution to the diffusion equation for an initial step function, namely, according to the well-known complementary error function solution (see pp 79-81 of [2] and specifically Figure 3.4). Later, the structure during the "birth of the reaction zone", as Kapila calls it, occurs. During this phase, there are outer regions where the fuel and oxidizer remain undisturbed, and these are characterized, as described above, by the reaction being zero so that there is either all fuel or all oxidizer, as we have noted from Eq. (23). Kapila then determines the inner region, where both the fuel and the oxidizer make the transition from their outer-region values continuously to zero (see pp 81-82). Finally, there is an inner-inner region where the flame structure is detemined by a full transient reaction-diffusion balance. By rescaling variables, Kapila reduces this problem to one reported earlier in the literature [11]. Finally, by variable rescalings, the solution to the 1-D problem for later times when all three terms in the 1-D equation must be retained in the analysis is again reduced to that obtained by Friedlander and Keller [11]. It should be noted that both the inner-inner structure and the later-time solutions cannot be evaluated by analytical means, but require numerical evaluation.

For early times, Eqs. (23) and (24) simplify considerably, reducing to the 1-D problem discussed above over large regions of the solution plane. In the first subsections below, an approximate solution in terms of special functions is presented for early times and the consumption rate at early time is calculated. In later subsections, we discuss the long-time solution or fast reaction case, relating the results to those obtained by Kapila, and calculate the consumption rate from the long-time solution. Generally, we have chosen to determine the solution to Eq.(23) directly by numerical methods, and these results are presented in the last section.

4.1 Slow Reaction

We examine this equation in the limit of small time or small reaction rate. In this case, we change dependent variables to

$$W(\mu, t) = t' H_0(\mu) \tag{25}$$

For small time $t' \ll 1$ and $\mathrm{Re}\, t'/\eta' \ll 1$,
$f_1 \to (1/3)(t'/\eta')^2, f \to 1/\sqrt{1 + (1/3)(\mathrm{Re}\, t'/\eta')^2}$ and $F \to 1 - (2/3)(\mathrm{Re}\, t'/\eta')^2$. Then the equation for H_0 reduces to the same equation one obtains in the one-dimensional problem discussed above, namely,

$$\frac{d^2 H_0}{d\mu^2} + 2\mu \frac{dH_0}{d\mu} - 4H_0(\mu) = 4Z(\mu)[1 - Z(\mu)] \tag{26}$$

and this equation has an analytical solution in terms of special functions. The solution is

$$H_0(\zeta) = a_+(\zeta) H_+(\zeta) + a_-(\zeta) H_-(\zeta) \tag{27}$$

where

$$a_+(\zeta) = -2\sqrt{\pi} \int_{-\infty}^{\zeta} d\xi \exp(\xi^2) H_-(\xi)[1 - \mathrm{erf}^2(\xi)]$$

$$a_-(\zeta) = -2\sqrt{\pi}\int_\zeta^\infty d\xi \exp(\xi^2) H_+(\xi)[1 - \mathrm{erf}^2(\xi)]$$

$$H_+(\zeta) = (1/2)(\zeta^2 + 1/2)\,\mathrm{erfc}\,(\zeta) - \frac{\zeta}{2\sqrt{\pi}}\exp(-\zeta^2)$$

$$H_-(\zeta) = (1/2)(\zeta^2 + 1/2)\,\mathrm{erfc}\,(-\zeta) + \frac{\zeta}{2\sqrt{\pi}}\exp(-\zeta^2) \tag{28}$$

The condition $t' \ll 1$ is simply a statement that time is small relative to the chemical reaction-rate time. The second condition, $\mathrm{Re}\, t'/\eta' \ll 1$, on the other hand, is a condition relating the Reynolds number and the radius at the time under consideration. It states that, for a given vorticity or circulation (or Reynolds number), the radius cannot be too small or the approximation will be invalid. The solution for H_0 gives the slope of the solution for W at early time. It is interesting that, once again, in this limit, the full 2-D problem reduces to the 1-D one. The numerical results presented in the next section show that the early-time behavior does indeed look like a 1-D problem.

4.2 Consumption Rate for Slow Reactions

Here, we will concern ourselves on the calculation of the consumption rate at early times. The consumption rate is calculated directly by integration over the plane of the local reaction rate term

$$\langle R \rangle = \int_0^{2\pi} d\theta \int_0^\infty r dr R(r, \theta, t) \tag{29}$$

where

$$R = \tilde{k} Y_{10} Y_{20} (Z + W)(1 - Z + W) \tag{30}$$

Performing all of the transformations of variables, this integral can be written

$$\langle R \rangle = 4 Y_{10} D\,\mathrm{Sc} \int_0^\infty d\eta'' \int_0^1 \frac{d\mu}{\sqrt{1-\mu^2}} \left[\tilde{R}_+ + \tilde{R}_-\right] \tag{31}$$

where $\tilde{R}(\mu, \eta'', t')$ and $\tilde{R}_\pm$ denotes $\tilde{R}(\pm\xi', \eta'', t')$ where $\xi' = f(\eta''/t')\sqrt{\mathrm{Sc}\,\eta''/t'}\mu$.

Now for small time, as noted above, W is proportional to time, so that for early time, $|W| \ll |Z|$, and we can approximate the local reaction rate by $\tilde{k} Z(1 - Z)$. If we now integrate by parts, and make one additional simplification (not required, but useful) that $\sin^{-1}(\mu) \approx (\pi/2)\mu$, then

$$\langle R \rangle \approx 4 Y_{10} D\,\mathrm{Sc}\, t' [\pi/4 J_1(\mathrm{Re}, \mathrm{Sc}) + 2/\sqrt{\pi} J_2(\mathrm{Re}, \mathrm{Sc})] \tag{32}$$

where

$$J_1 = \int_0^\infty d\eta' [1 - \mathrm{erf}^2(\xi)]$$

$$J_2 = \int_0^\infty d\eta' (\pi/\xi)[\mathrm{erf}\,(\sqrt{2}\xi)/(\sqrt{2}\xi) - \mathrm{erf}\,(\xi)\exp(-\xi^2)] \tag{33}$$

where $\xi = f(\eta')\sqrt{\mathrm{Sc}\,\eta'}$, and from these integrals, the parametric dependences upon the Reynolds number and the Schmidt number can be assessed. The first observation that can

be made about the consumption rate is that it is proportional to time; i.e., the rate of reaction of the species increases linearly with time at early time. This behavior is to be contrasted with that of a fast reaction, or late time, where the consumption rate is constant as a function of time.

4.3 Fast Reaction

When the time is long or the reaction fast, then over much of the solution plane there is still either fuel or oxidizer and no reaction, as noted earlier. Furthermore, the solution very quickly passes over approximately to the flame-sheet or infinite-rate-chemistry case everywhere except near the flame front (as will be shown by examples in Section 5). Only in the reaction region near the z-axis and around the winding reaction front will there be variations from the flame-sheet solution.

The reaction-zone structure can be related to the results given by Kapila [2]. Here, we simply state his results in terms of our formulation and notation in the 1-D case. If we change the independent variable from μ to ξ and the independent variable from W to $\tilde{W}$ as follows

$$\begin{aligned} \mu &= \xi t^{-\lambda} \\ W &= -(1/2) + t^{-\lambda}\tilde{W} \end{aligned} \tag{34}$$

Then $\text{erf}\,(\xi t^{-\lambda}) \rightarrow \frac{2}{\sqrt{\pi}}\xi t^{-\lambda}$ and, as Kapila [2] finds, $\lambda = 1/3$. The equation for $\tilde{W}$ is

$$\frac{d^2\tilde{W}}{d\xi^2} = 4(\tilde{W} - \frac{\xi}{\sqrt{\pi}})(\tilde{W} + \frac{\xi}{\sqrt{\pi}}) \tag{35}$$

(Some numerical factors do not agree between the two formulations.) The solution for this equation was solved earlier by Friedlander and Keller [11].

4.4 Consumption Rate for Fast Reactions

The consumption rate for a stoichiometric mixture was calculated originally by Marble [3] and by alternate means by Rehm et al [8] to obtain the parametric dependences of this rate upon Reynolds and Schmidt numbers. Here, we use the expressions derived above to calculate the consumption rate in the flame-sheet limit, specializing again to the case of a stoichiometric mixture for simplicity. However, with the expressions derived above, this specialization is not necessary.

We begin with the solution for the mixture fraction Eq.(20) and the definition of the independent variable μ, Eq.(17). At the flame sheet, the constant $Z(\mu_f) = Z_f$ contour is determined as a constant $\mu = \mu_f$ curve. Along the the flame sheet, θ_0 is a function of η, and through the transformation between Eulerian and Lagrangian coordinates, we determine $\theta(\eta)$ and the derivative $rd\theta/dr$. The consumption rate is proportional to the normal derivative of the mixture fraction along the flame sheet,

$$\frac{\partial Z}{\partial n} = \vec{i}_n \cdot \nabla Z$$

$$= \frac{dZ}{d\mu} \vec{i}_n \cdot \nabla \mu$$

For the special case of a stoichiometric mixture, $\mu_f = 0$, and the algebra simplifies considerably. In this case, the integral of the normal derivative of the mixture fraction along the flame sheet simplifies to the expression

$$\int \left(\frac{\partial Z}{\partial n}\right)_f ds = \frac{2\sqrt{\mathrm{Sc}}}{\sqrt{\pi}} \int_0^\infty \frac{f(\eta)}{\sqrt{\eta}} \left[1 + \frac{\mathrm{Re}^2}{\eta^2}(1 - \exp(-\eta))^2\right] d\eta \tag{36}$$

An observation about this integral is in order. When the Reynolds number is set to zero, so that no mixing occurs, the one-dimensional case is recovered. In this case, $f(\eta) = 1$, and the integrand is simply the reciprocal of the square root of η, which when integrated over the infinite interval, is infinite. This unbounded integral arises from the fact that the flame sheet is infinite, and, therefore, the consumption rate is unbounded. It can be eliminated by only calculating the enhancement in the consumption rate produced by the vortex mixing, as noted in previous analyses[3], [8]. When this is done, we can obtain the enhancement in the consumption rate for all values of the Reynolds number (for large values of the Schmidt number). However, when the Reynolds number is large, the enhancement is obtained by eliminating the first term in the square bracket, replacing $f(\eta)$ by its asymptotic form for large Reynolds number, and integrating from the inner core (where burning has ceased) to infinity. The lower limit of integration is determined by $\eta_c = (\mu_c \,\mathrm{Re}/\sqrt{3\,\mathrm{Sc}})^{2/3}$ where $\mu_c << 1$ specifies the inner core, where $Z(\mu) \approx 1/2$. The enhancement is found to be proportional to $(\,\mathrm{Re}\,\mathrm{Sc}\,)^{2/3}$, as determined in earlier analyses.

5 Numerical Results

In this section, we show results both for the flame-sheet solution and for the finite-rate chemistry solution in the large-Schmidt-number approximation. Results determined from the expressions derived in Section 3 are compared with those determined by methods described in [8] also making a large-Schmidt-number approximation. As noted earlier, the approximate solution described in Section 3 is much simpler than that obtained earlier [8], and this simpler solution (and the transformation used to obtain it) allow one to carry the analysis in the finite-rate-chemistry case much further.

In Figure 2a are shown contours of constant mixture-fraction variable Z in the Lagrangian coordinate system as a function of ρ and θ_0. These contours were determined using the methods described in [8] and are for $\mathrm{Re} = 100$, $\mathrm{Sc} = 10$. (For display purposes, the data was generated on a 151^2 grid.) The contours are for $|Z - 0.5| = \epsilon, 0.1, 0.2, 0.3, 0.4$ with $\epsilon = 10^{-2}$. The contours $Z = 0.5 \pm 10^{-2}$ are close to the critical one for stoichiometry, and these contours in Lagrangian coordinates remain close to the y-axis away from the origin and broaden due to combustion to a flat circular region around the origin. In Figure 2b is shown the same set of contours, but with $\epsilon = 10^{-4}$. In Figure 2d is shown the same set of contours, but with $\epsilon = 0.0$. Note that the contour for $|Z - 0.5| = 0.0$ behaves in an unusual, not symmetrical fashion; it is not correct. As shown in [12], this behavior is a result of numerical underflow in computing the asymptotic expressions in [8]. In Figure 2c is shown the same

set of contours with $\epsilon = 0.0$ but computed using symmetric level index (sli) arithmetic [13]. Sli is a methodology for computing quantities over a much wider dynamical range than is usually available in standard computer arithmetic. With sli, numerical underflows can be significantly reduced, and this procedure was used to determine results for Fig. 2c [12]. These contours are correct.

Figures 3a through 3d show the same contours as those shown in Figures 2a through 2d and calculated in the same way, but in Eulerian coordinates. The contours in Eulerian coordinates display the winding which is characteristic of the process and difficult to compute accurately by standard numerical methods. The incorrect behavior exhibited in Fig. 2d is reflected in Fig. 3d; compare the correct behavior shown in Fig. 3c.

Each contour in Figures 2 and 3 represents a flame sheet for a different value of the mixture fraction initially (or a different value of $\alpha = Y_{10}/Y_{20}$). As noted earlier, only for stoichiometry does the flame sheet remain along the y-axis far from the origin; for other values of the mixture fraction initially, the flame sheet either follows a contour on the fuel-rich side ($1/2 \leq Z \leq 1$) or on the fuel-lean side ($0 \leq Z \leq 1/2$). Therefore, when each of these contours is displayed in Eulerian coordinates, it represents a flame sheet for an appropriate initial mixture fraction in the laboratory reference frame.

Figures 4 and 5 show the same contours displayed in Figures 2 and 3 respectively, but calculated using the asymptotic expressions obtained in Section 3. In Figs. 4a and 5a, the contours are shown for $\epsilon = 10^{-2}$ while in Figs. 4b and 5b, the contours are for $\epsilon = 0.0$; the contours for $\epsilon = 10^{-4}$ are indistinguishable from those for $\epsilon = 0.0$ in each case. These figures were generated using sli. However, for the expressions derived in Section 3, the underflow does not occur and, therefore, correct contours are generated using standard computer arithmetic.

Only in Figures 4a and 4b, where the contours are displayed in Lagrangian coordinates, can any significant differences between the two asymptotic expressions be seen, and then only in the neighborhood of the origin. The most apparent difference is that the contours are symmetric with respect to the x-axis using the expressions derived in Section 3, whereas they are not in the expressions derived in [8]. For the purpose of calculating the reaction-rate enhancement due to vortex mixing, these differences are relatively small since near the origin, where the differences are largest, the reaction rate has been significantly reduced due to the mixing and diffusion.

For finite-rate chemistry, we show results at a few times for only one set of parameters assuming large Reynolds and Schmidt numbers and stoichiometry, Re = 100, Sc = 10, and $\alpha = 1$. In Figure 6, four plots of W are shown at dimensionless times t'=20.4, 152, 1136 and 3103 as computed from Eq.(23) over a 10x10 region of the η plane and plotted by evaluating W on a grid and using NCAR graphics. The deviation of the species from that found using flame-sheet analysis, W, is found to change from its initial value, zero, to its minimum value, -0.5, as a spiral that slowly winds up and expands out into the plane, indicating how the structure of the combustion zone changes in physical space as time progresses. It should be noted that in the core of the expanding spiral region, the value of W becomes zero again where the reaction is complete. As noted in the last section, for early times, there is only a reaction-diffusion balance; convection has not had time to develop and to distort this balance. For the scale used here, this balance is the appropriate one everywhere except near the origin. Therefore, in the plot of W, even up to a few units of time, W is essentially zero

everywhere except along the z-axis and within about a unit of the origin, where only slight rotational distortion has begun to occur. For comparison, Z, the mixture-fraction variable is shown at the same four times in Figure 7. The reaction rate at these times is shown in Figure 8, showing how the structure of the reaction zone developes as time progresses.

In Fig. 9, the reaction rate at several times is contrasted for (a) stoichiometry ($\alpha = 1.0$) versus (b) nonstoichiometry ($\alpha = 0.5$). The reaction rate is plotted at a specified value of η, or radius, as a function of μ, the coordinate normal to the flame front, for eight times in each case. Note that the reaction is skewed toward the fuel-rich side for $\alpha = 0.5$ compared to the symmetric case of $\alpha = 1.0$.

Finally, in Figure 10 is shown the result of plotting Y_1/Y_{10} and Y_2/Y_{20} versus Z at many spatial points for three different times. At relatively early time, the concentration ratios for each species vary smoothly from zero to one with mostly fuel on the fuel side and mostly oxidizer on the other, but some of each on both sides of the reaction zone. At later times, however, the region of orerlap where both fuel and oxidizer are nonzero decreases. Finally, at the last time, a state relation develops in which the relative concentration depends only upon Z and not on time, and only fuel is found to the left of the flame while only oxidizer is found to the right. Also, the flame structure has collapsed to a flame sheet.

6 Acknowledgments

The first author wishes to thank Professor John Ockendon and the Mathematical Institute of the University of Oxford for the hospitality shown to him when he visited during the Spring of 1989; part of this work was done at that time.

References

[1] Carrier, G.F., Fendell, F.E. and Marble, F.E., "The Effect of Strain Rate on Diffusion Flames", SIAM J. Appl. Math., Vol. 28, No.2, March, 1975, p. 453.

[2] Kapila, A.K., *Asymptotic Treatment of Chemically Reacting Systems*, Pitman Advanced Publishing Program, Boston 1983, pp 77-91.

[3] Marble, F.E., "Growth of a Diffusion Flame in the Field of a Vortex", *Recent Advances in Aerospace Sciences* (C. Cassci, Ed.) 1985, p. 315.

[4] Baum, H.R., Corley, D.M. and Rehm, R.G., "Time-Dependent Simulation of Small-Scale Turbulent Mixing and Reaction", Twenty First Symposium (International) on Combustion, The Combustion Institute, pp 1263-1270.

[5] Karagozian, A.R. and Marble, F.E., "Study of a Diffusion Flame in a Stretched Vortex", Comb. Sci. Tech., Vol. 45, 1986, p. 65.

[6] Karagozian, A.R., "An Analytical Study of Diffusion Flames in Vortex Structures", Ph.D. Thesis, California Institute of Technology, Pasadena, Cal. (1982).

[7] Norton, O.P., "The Effects of a Vortex Field on Flames with Finite Reaction Rates", Ph.D. Thesis, California Institute of Technology, Pasadena, CA, 1983.

[8] Rehm, R.G., Baum, H.R., Lozier, D.W. and Aronson, J., "Diffusion-Controlled Reaction in a Vortex Field", Combustion Science and Technology, Vol. 66, No. 4-6, p 293 (1989).

[9] Dahm, W.J.A., and Buch, K.A., "High Resolution Three-Dimensional (256^3) Spatio-Temporal Measurements of Conserved Scalalr Field in Turbulent Shear Flows", University of Michigan, Department of Aerospace Engineering, Report No. GRI-5087-260-1443-4 (1989).

[10] Williams, F.A., *Combustion Theory*, Second Edition, The Benjamin/Cummings Publishing Co., Menlo Park, CA, 1985.

[11] Friedlander, S.K., and Keller, K.H., "The Structure of the Zone of Diffusion-Controlled Reaction", *Chem. Engng. Sci.*, 18, p 365.

[12] Lozier, D.W., "An Underflow-Induced Graphics Failure" paper to be submitted for publication.

[13] Clenshaw, C.W., Olver, F.W.J. and Turner, P.R., "Level-Index Arithmetic: An Introductory Survey," in Numerical Analysis and Parallel Processing, Lecture Notes in Mathematics 1397, P.R. Turner, Ed., Springer-Verlag, 1989, pp. 95-168.

Figure Captions

Figure 1. Schematic diagram of vortex, flame-sheet interaction.

Figure 2.a. Contours of constant mixture-fraction variable Z in Lagrangian coordinates for Re $= 100$, Sc $= 10$ using the asymptotic epressions from [8]. The contours are for $|Z = -0.5| = \epsilon$, 0.1, 0.2, 0.3, 0.4 with $\epsilon = 10^{-2}$.

Figure 2.b. Contours of constant mixture-fraction variable Z in Lagrangian coordinates for Re $= 100$, Sc $= 10$ using the asymptotic epressions from [8]. The contours are for $|Z = -0.5| = \epsilon$, 0.1, 0.2, 0.3, 0.4 with $\epsilon = 10^{-4}$.

Figure 2.c. Contours of constant mixture-fraction variable Z in Lagrangian coordinates for Re $= 100$, Sc $= 10$ using the asymptotic epressions from [8]. The contours are for $|Z = -0.5| = \epsilon$, 0.1, 0.2, 0.3, 0.4 with $\epsilon = 0.0$, and symmetric-level-index arithmetic has been used to evaluate the asymptotic expression.

Figure 2.d. Contours of constant mixture-fraction variable Z in Lagrangian coordinates for Re $= 100$, Sc $= 10$ using the asymptotic epressions from [8]. The contours are for $|Z = -0.5| = \epsilon$, 0.1, 0.2, 0.3, 0.4 with $\epsilon = 0.0$, and standard arithmetic has been used to evaluate the asymptotic expression. Note that the graphical representation of the function is misleading.

Figure 3.a. Contours of constant mixture-fraction variable Z in Eulerian coordinates for Re $= 100$, Sc $= 10$ using the asymptotic epressions from [8]. The contours are for $|Z = -0.5| = \epsilon$, 0.1, 0.2, 0.3, 0.4 with $\epsilon = 10^{-2}$.

Figure 3.b. Contours of constant mixture-fraction variable Z in Eulerian coordinates for Re $= 100$, Sc $= 10$ using the asymptotic epressions from [8]. The contours are for $|Z = -0.5| = \epsilon$, 0.1, 0.2, 0.3, 0.4 with $\epsilon = 10^{-4}$.

Figure 3.c. Contours of constant mixture-fraction variable Z in Eulerian coordinates for Re $= 100$, Sc $= 10$ using the asymptotic epressions from [8]. The contours are for $|Z = -0.5| = \epsilon$, 0.1, 0.2, 0.3, 0.4 with $\epsilon = 0.0$, and symmetric-level-index arithmetic has been used to evaluate the asymptotic expression.

Figure 3.d. Contours of constant mixture-fraction variable Z in Eulerian coordinates for Re $= 100$, Sc $= 10$ using the asymptotic epressions from [8]. The contours are for $|Z = -0.5| = \epsilon$, 0.1, 0.2, 0.3, 0.4 with $\epsilon = 0.0$, and standard arithmetic has been used to evaluate the asymptotic expression.

Figure 4.a. Contours of constant mixture-fraction variable Z in Lagrangian coordinates for Re $= 100$, Sc $= 10$ using the asymptotic expressions given in Section 3. The contours are for $|Z = -0.5| = \epsilon$, 0.1, 0.2, 0.3, 0.4 with $\epsilon = 10^{-2}$.

Figure 4.b. Contours of constant mixture-fraction variable Z in Lagrangian coordinates for Re = 100, Sc = 10 using the asymptotiv expressions given in Section 3. The contours are for $|Z = -0.5| = \epsilon$, 0.1, 0.2, 0.3, 0.4 with $\epsilon = 0.0$.

Figure 5.a. Contours of constant mixture-fraction variable Z in Eulerian coordinates for Re = 100, Sc = 10 using the asymptotic expressions given in Section 3. The contours are for $|Z = -0.5| = \epsilon$, 0.1, 0.2, 0.3, 0.4 with $\epsilon = 10^{-2}$.

Figure 5.b. Contours of constant mixture-fraction variable Z in Eulerian coordinates for Re = 100, Sc = 10 using the asymptotic expressions given in Section 3. The contours are for $|Z = -0.5| = \epsilon$, 0.1, 0.2, 0.3, 0.4 with $\epsilon = 0.0$.

Figure 6. Plots of the variable W at four different times, t'=20.4, 152, 1136 and 3103, for the parameters Re = 100, Sc = 10 and $\alpha = 1$. W is defined as the dimensionless difference between species 1 and the mixture-fraction variable (see Eq.(6)).

Figure 7. Plots of the variable Z at four differenc times, t'=20.4, 152, 1136 and 3103, for the parameters Re = 100, Sc = 10 and $\alpha = 1$. Z is the mixture-fraction variable (see Eq.(3)).

Figure 8. Plots of the rate of reaction at four differenc times, t'=20.4, 152, 1136 and 3103, for the parameters Re = 100, Sc = 10 and $\alpha = 1$. The rate of reaction is given by the expression $(W + Z)(\alpha W + 1 - Z)$ (see the right side of Eq.(21) for example).

Figure 9.a. Plots of the rate of reaction as a function of μ, the coordinate normal to the flame front, for a fixed value of ν, the radius, at eight times, for Re = 100, Sc = 10 and $\alpha = 1$.

Figure 9.b. Plots of the rate of reaction as a function of μ, the coordinate normal to the flame front, for a fixed value of ν, the radius, at eight times, for Re = 100, Sc = 10 and $\alpha = 0.5$.

Figure 10. Plots of the variables Y_1/Y_{10} and Y_2/Y_{20} versus the mixture-fraction variable Z at three different times, $t' = 7.5, 20.4$, and 1136. The parameters for the plots are Re = 100, Sc = 10 and $\alpha = 0.5$.

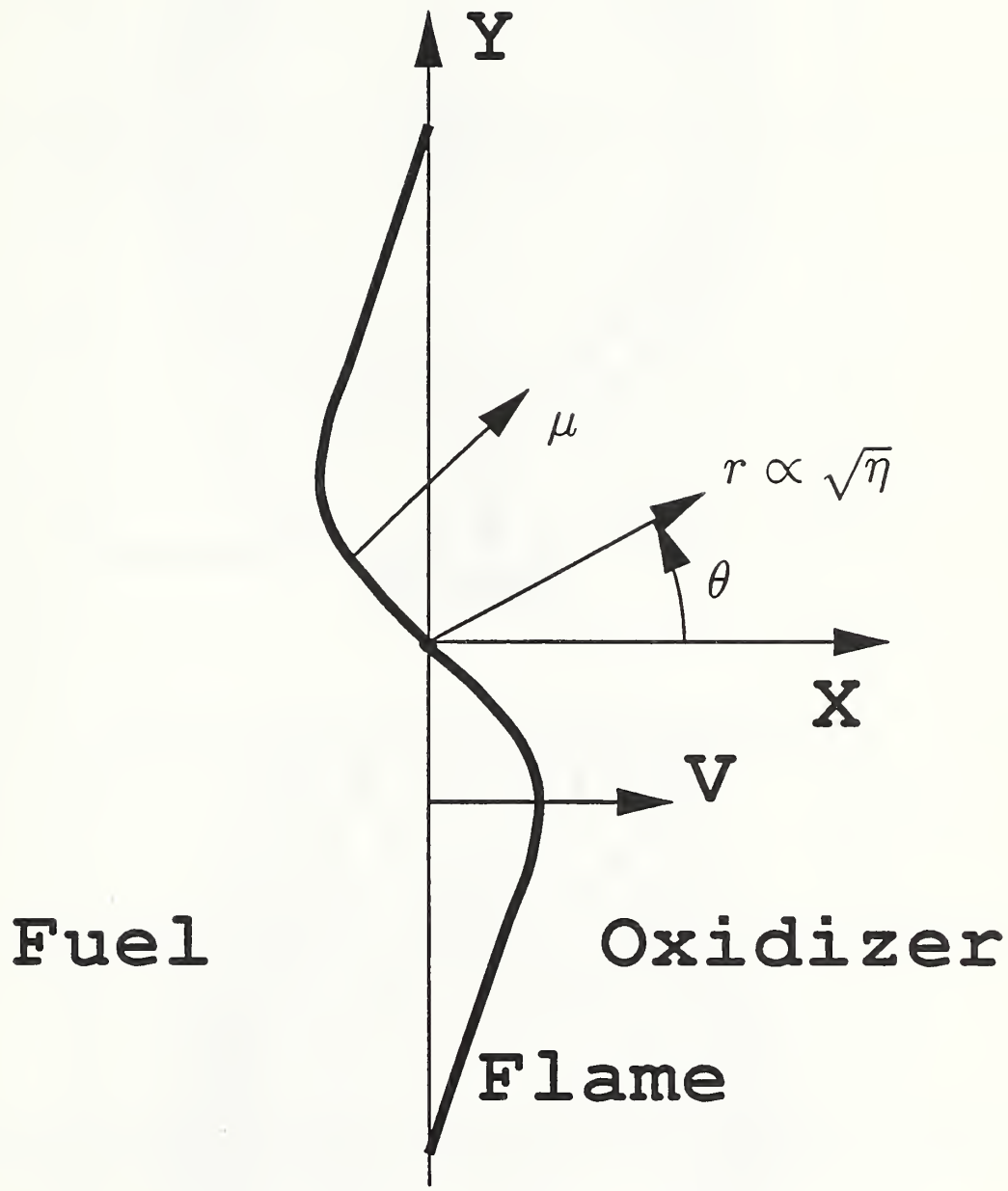

Figure 1

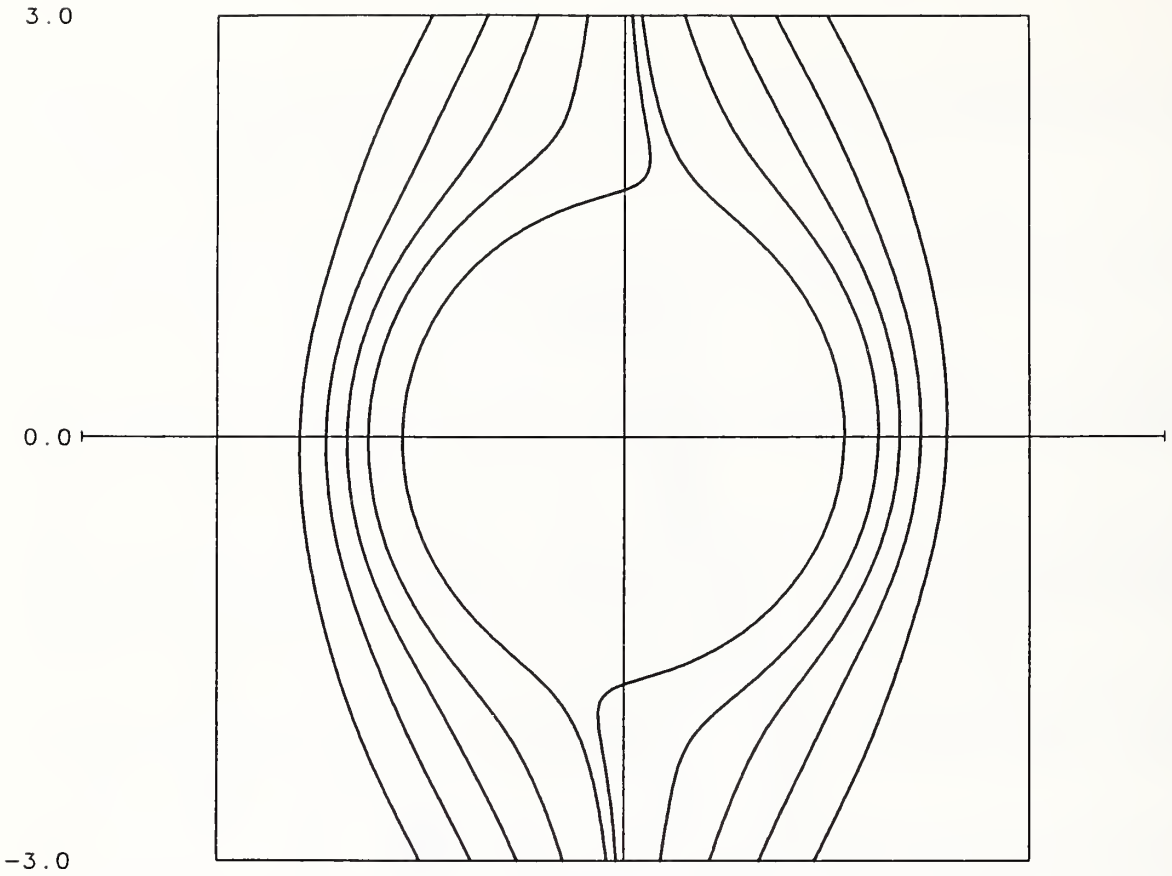

Figure 2a

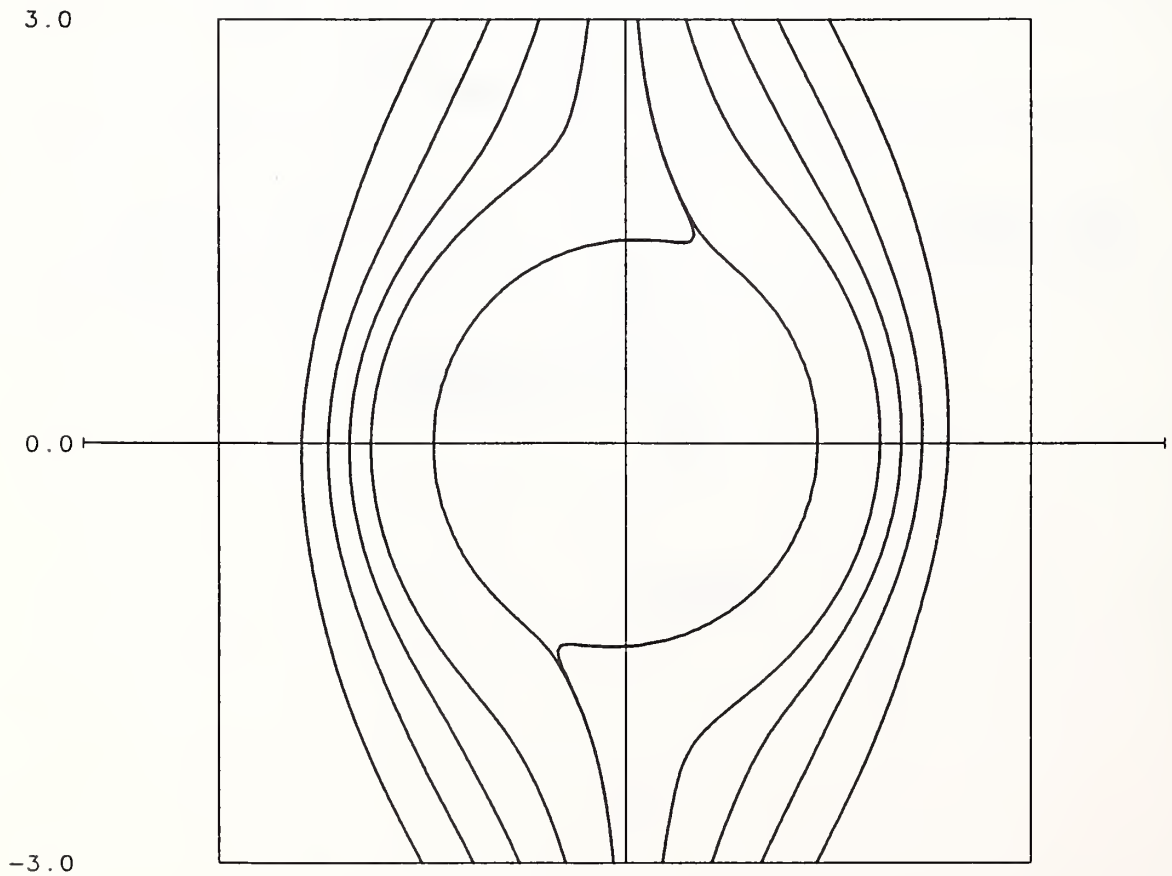

Figure 2b

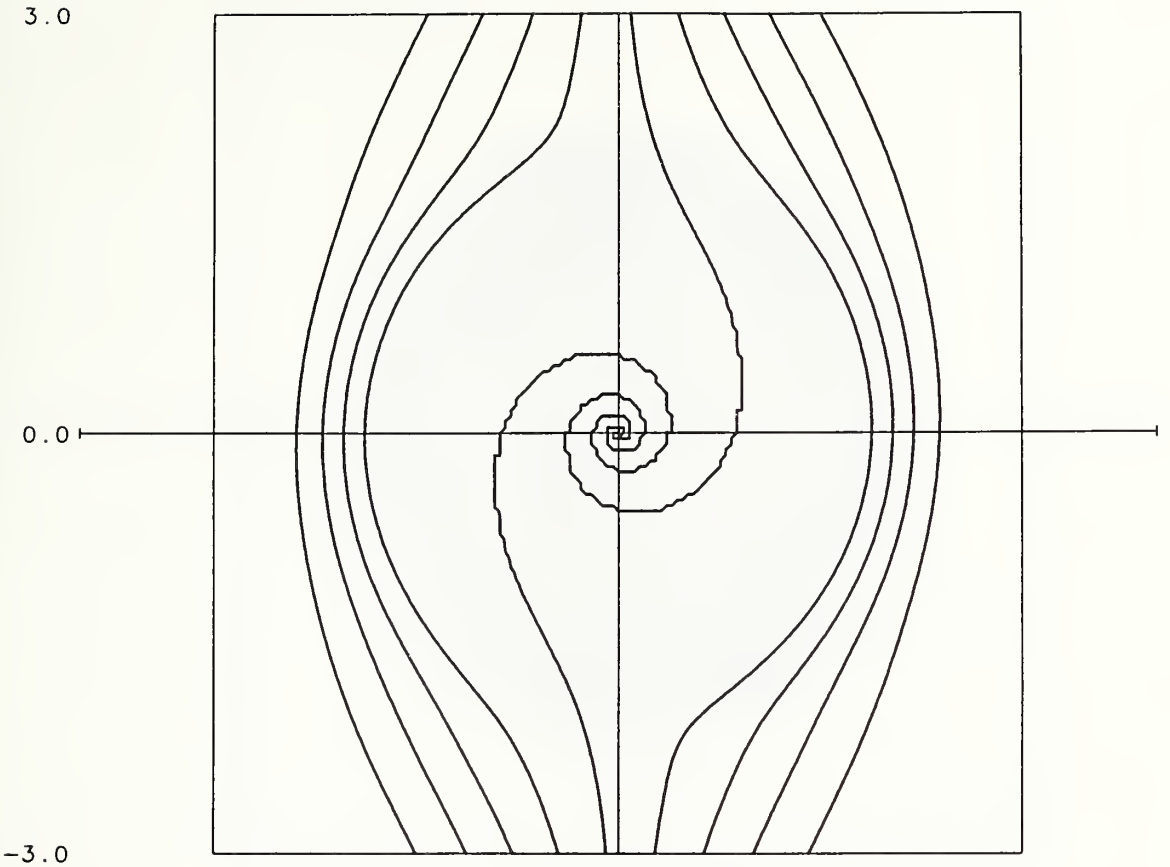

Figure 2c

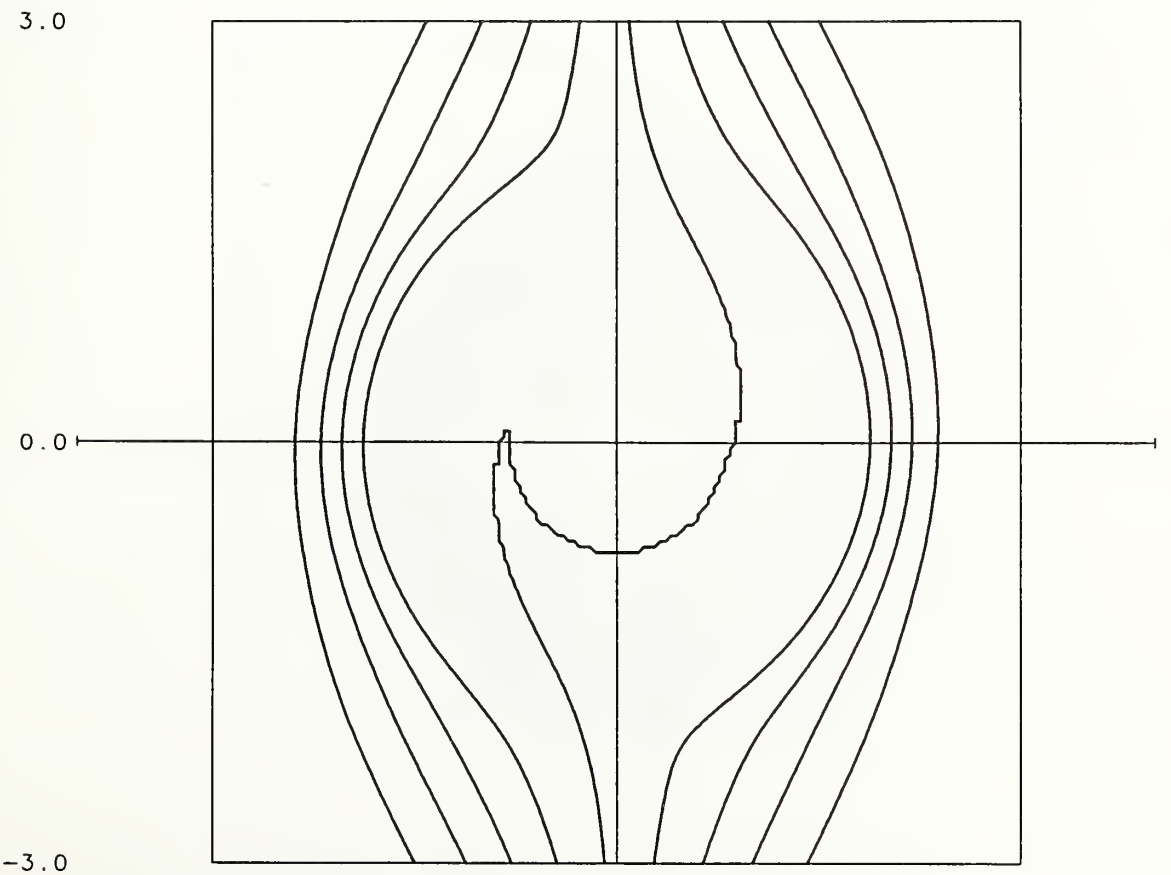

Figure 2d

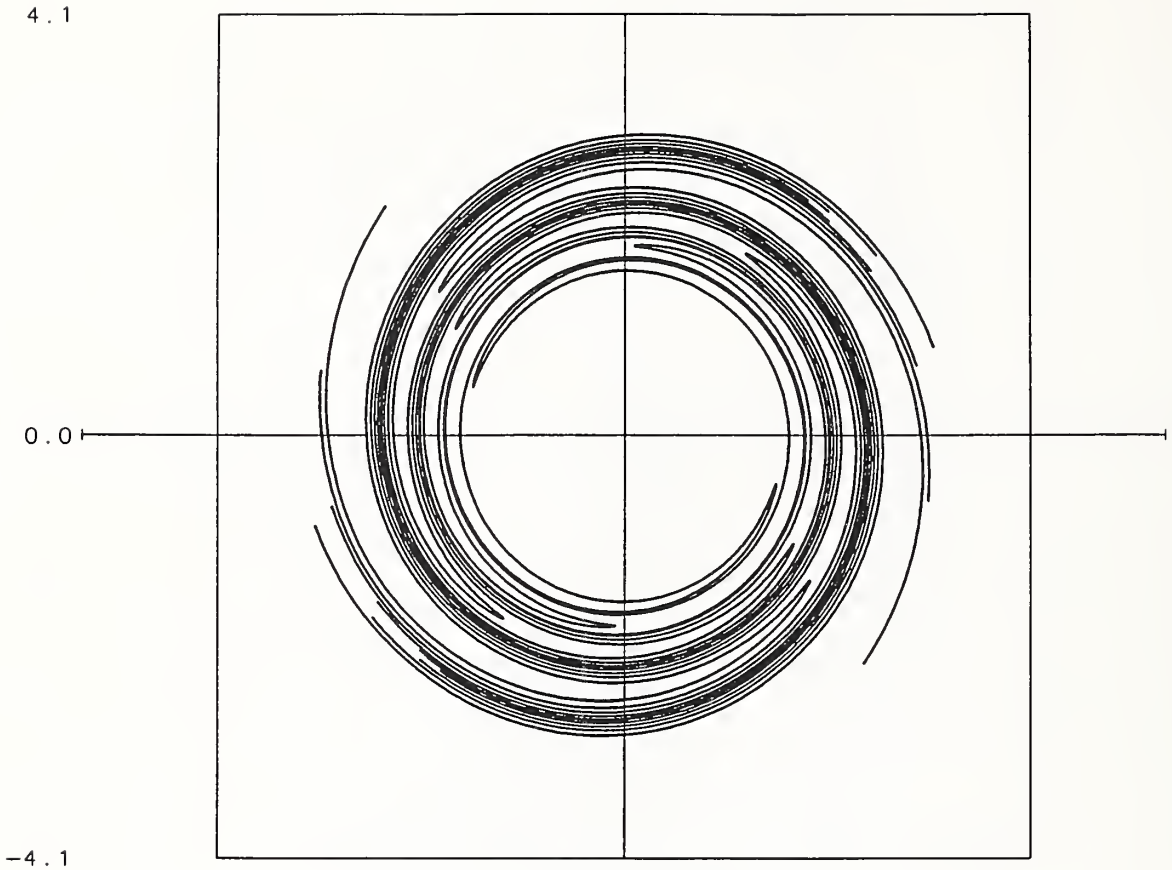

Figure 3a

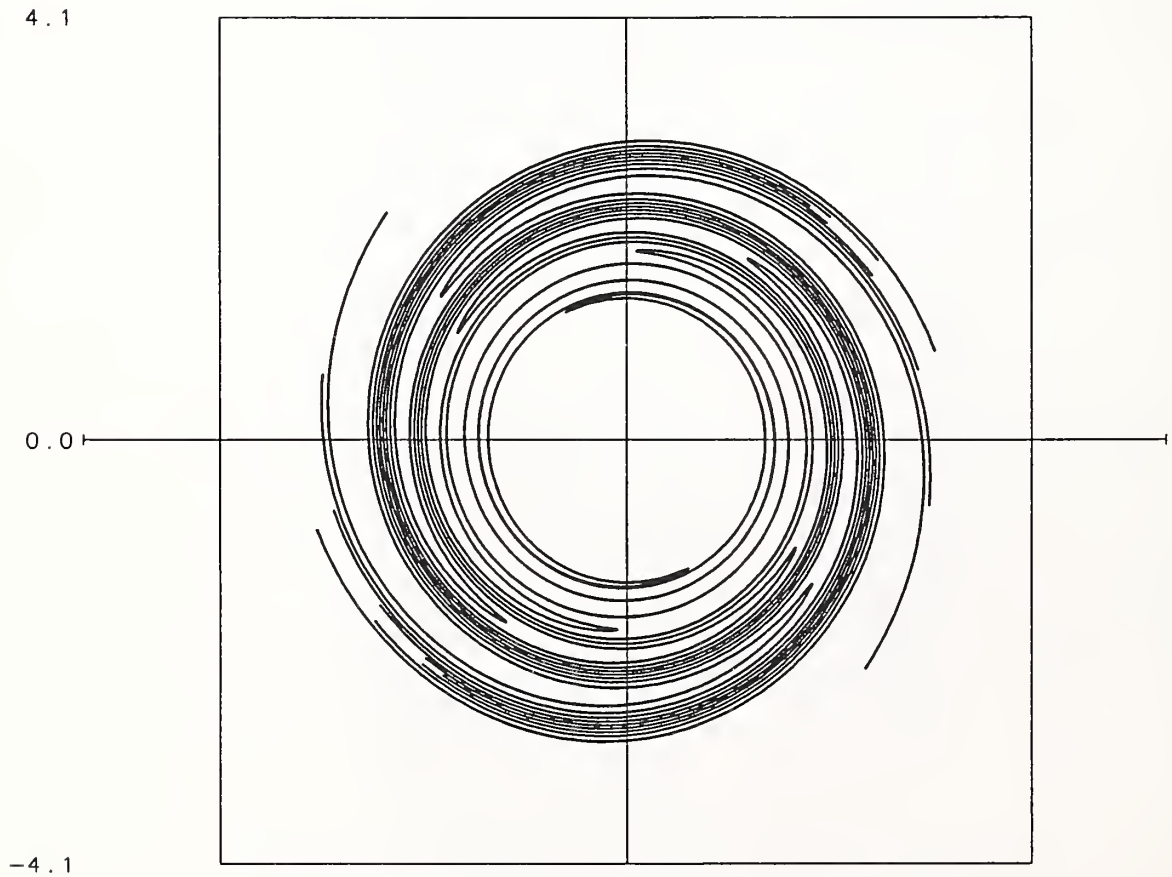

Figure 3b

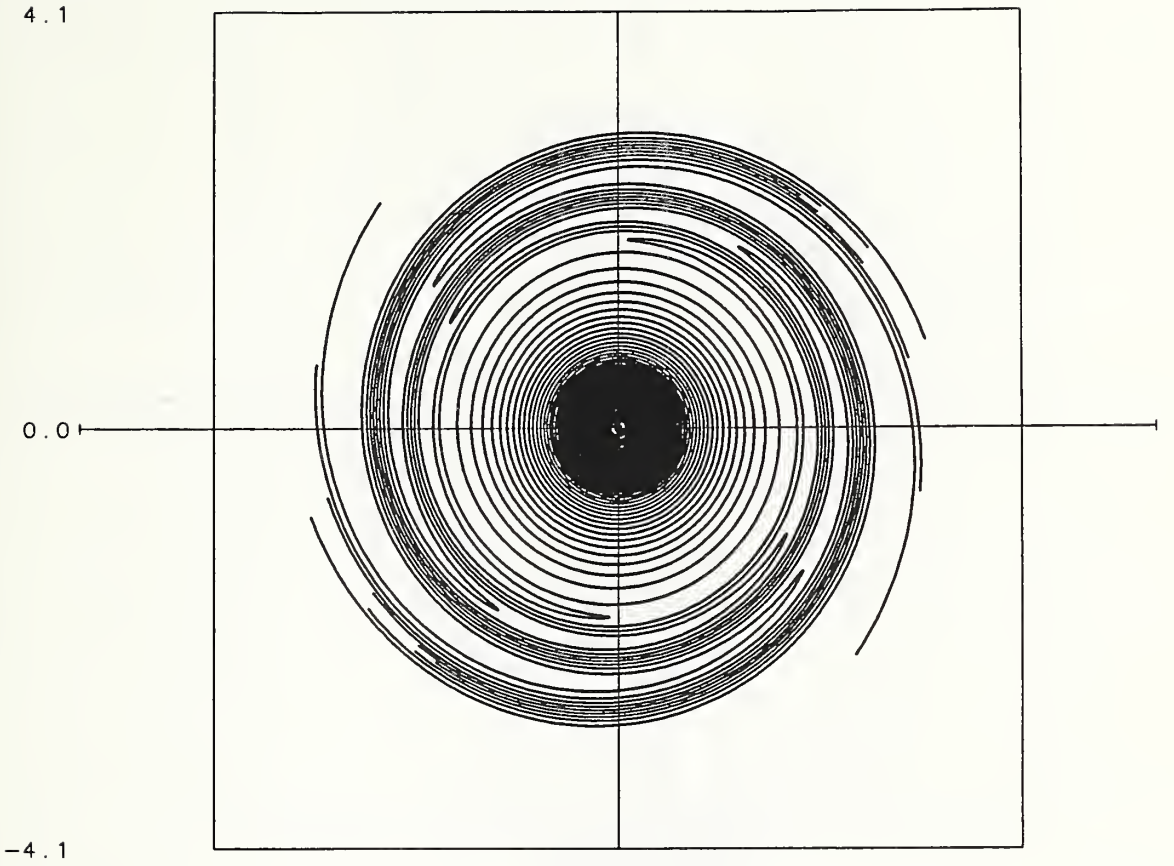

Figure 3c

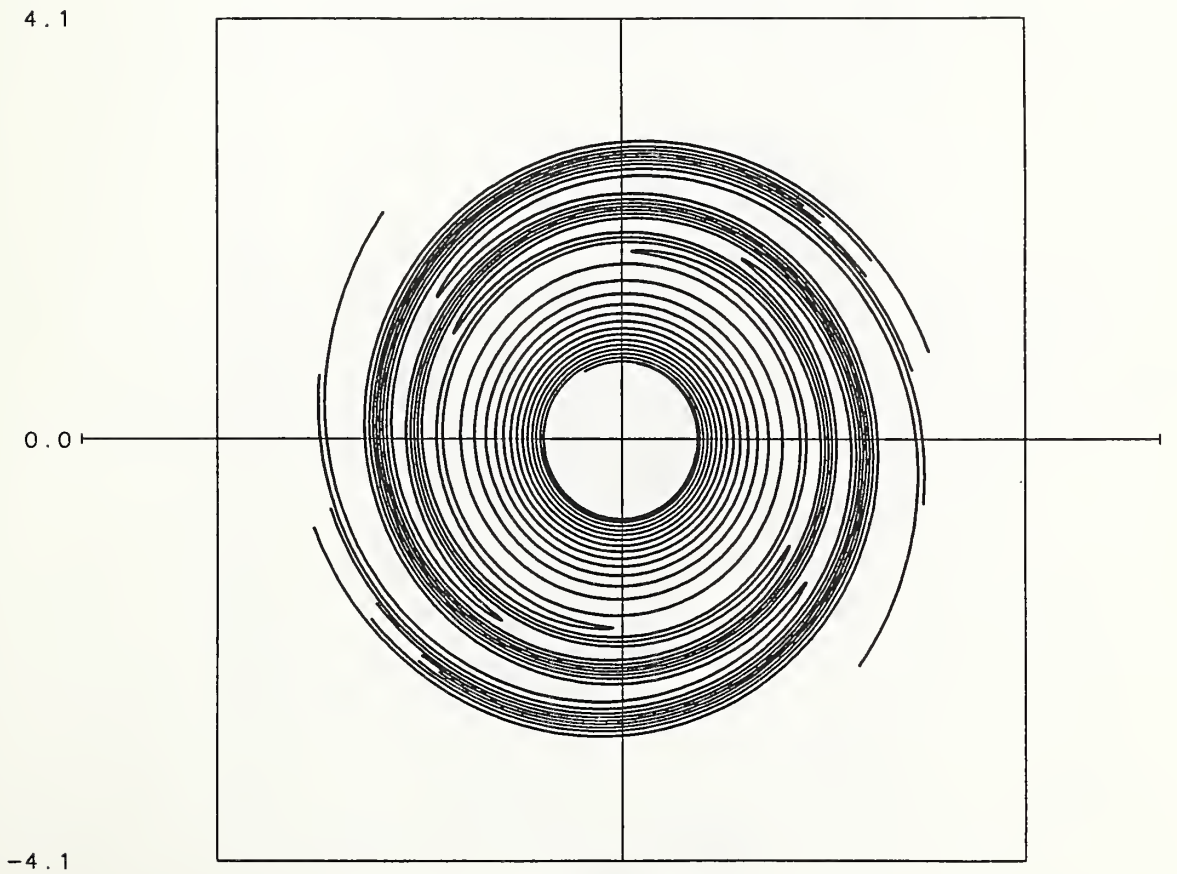

Figure 3d

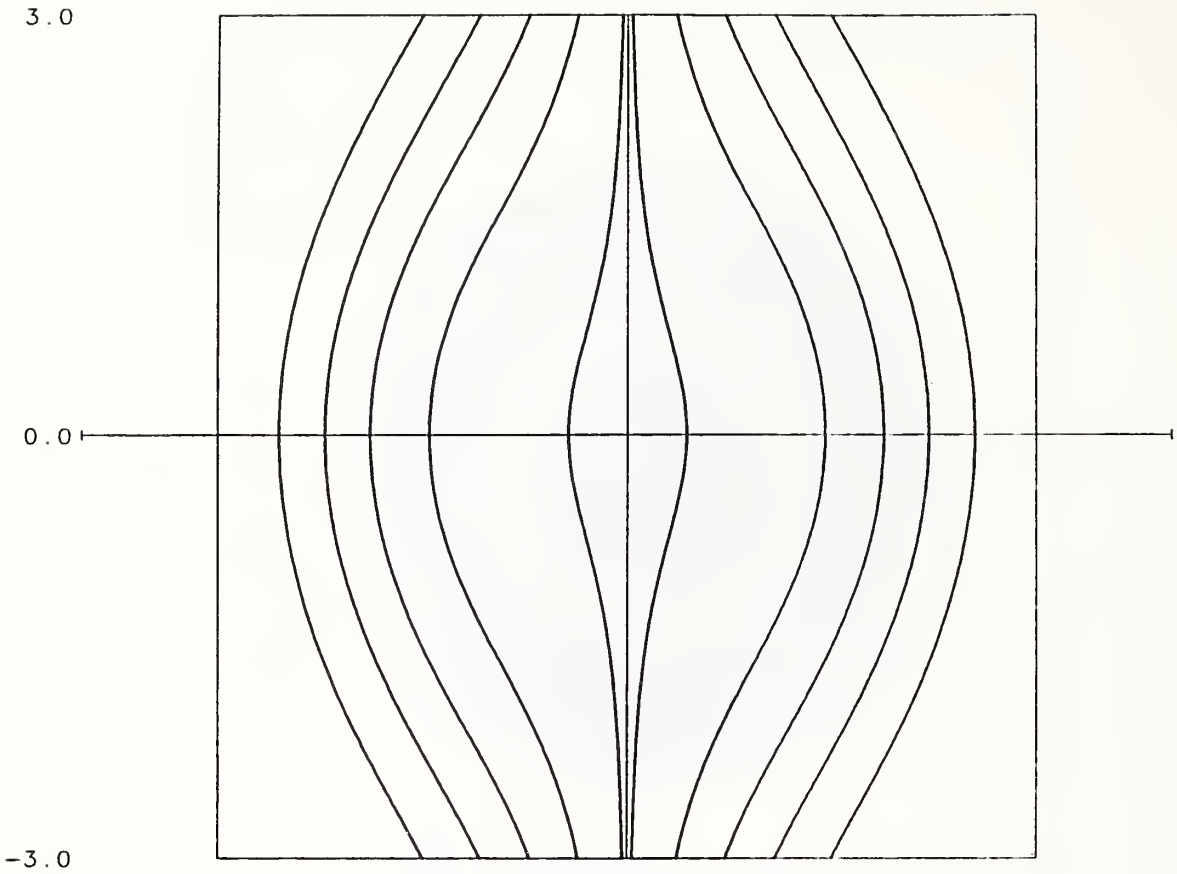

Figure 4a

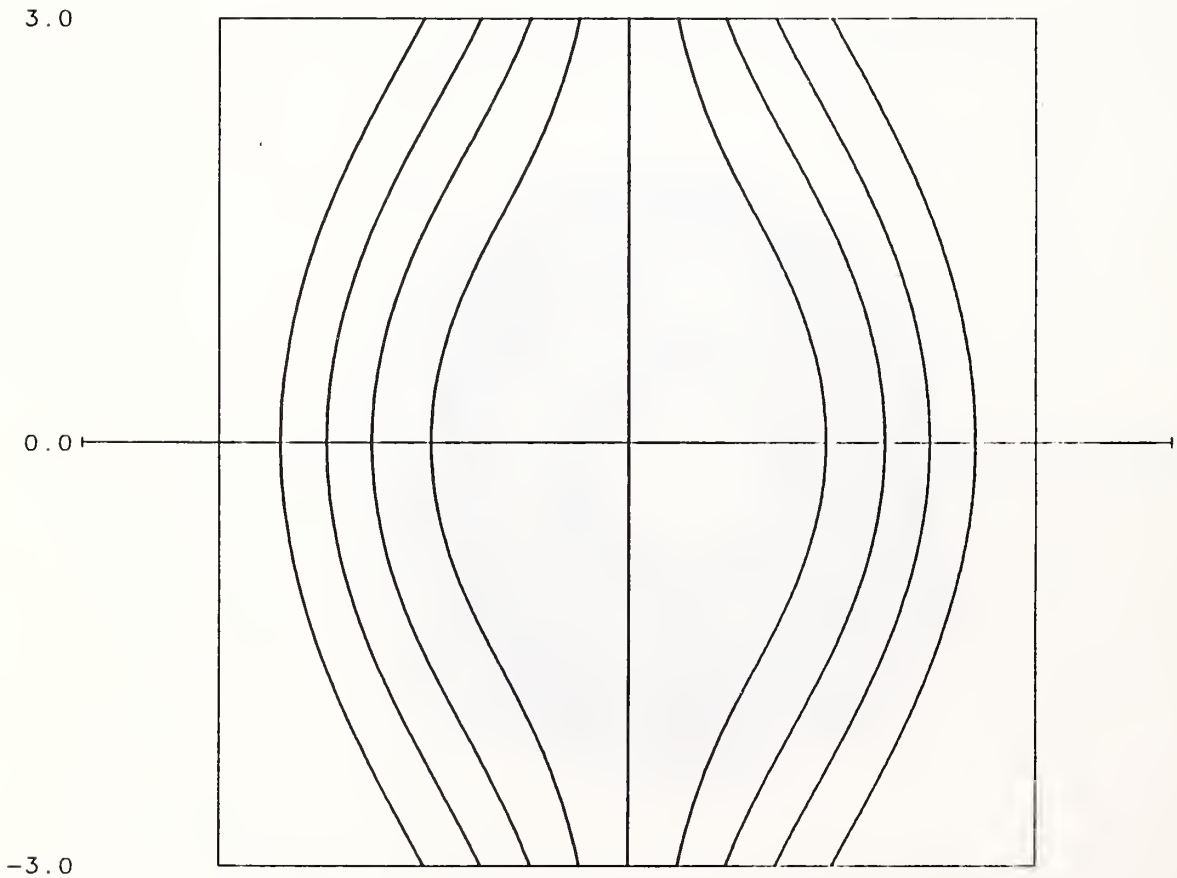

Figure 4b

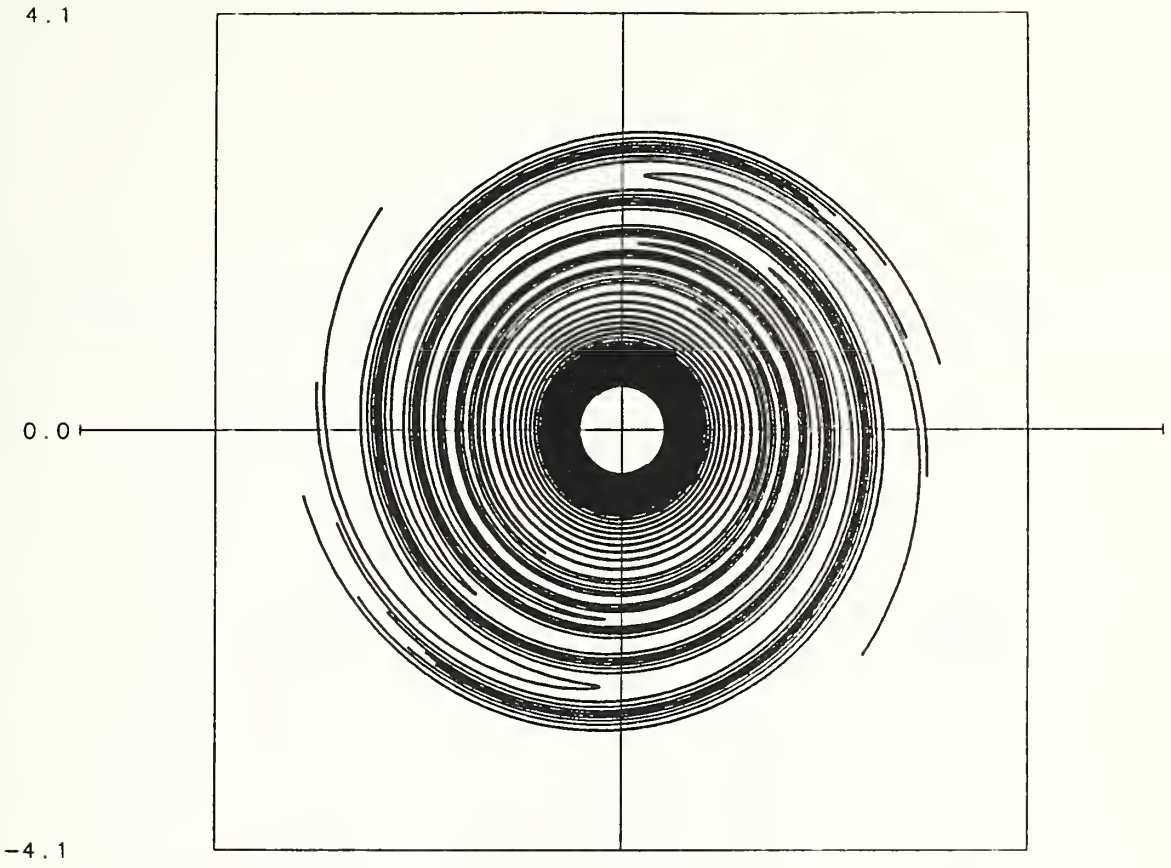

Figure 5a

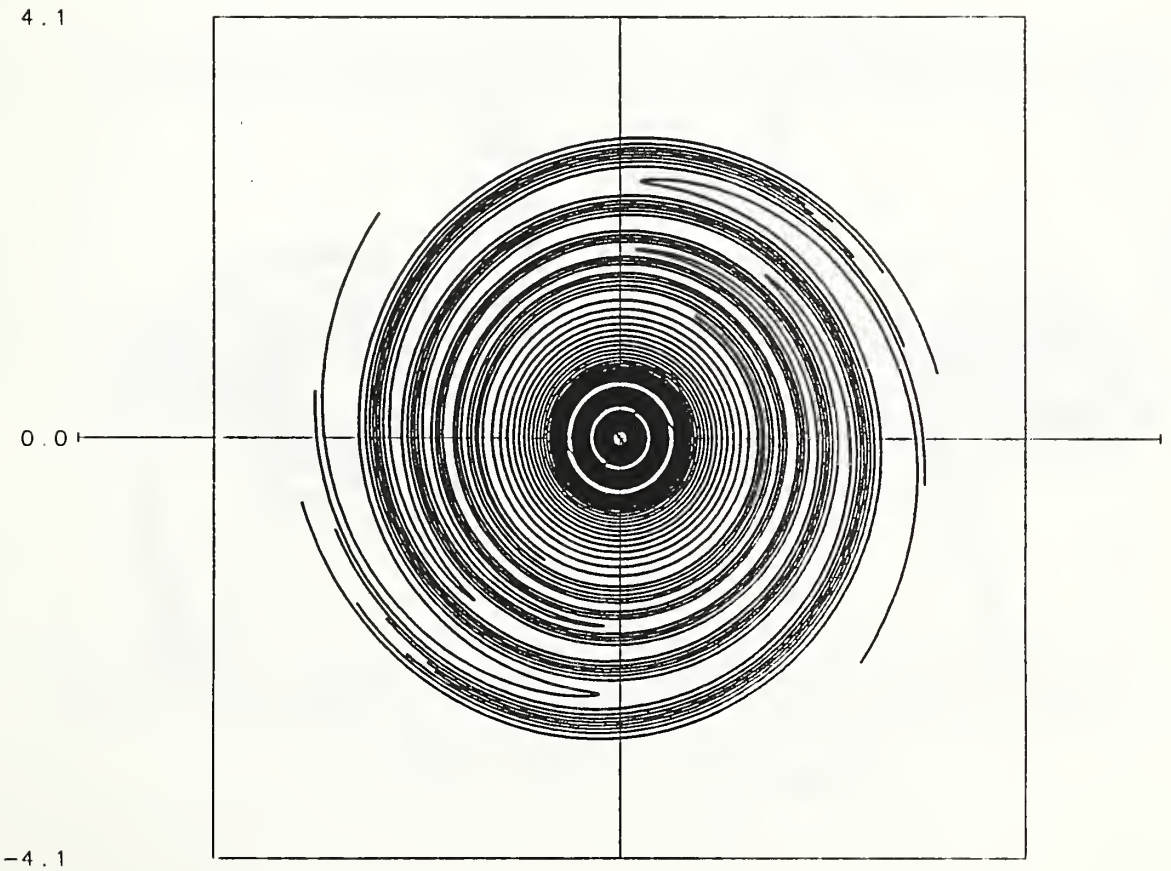

Figure 5b

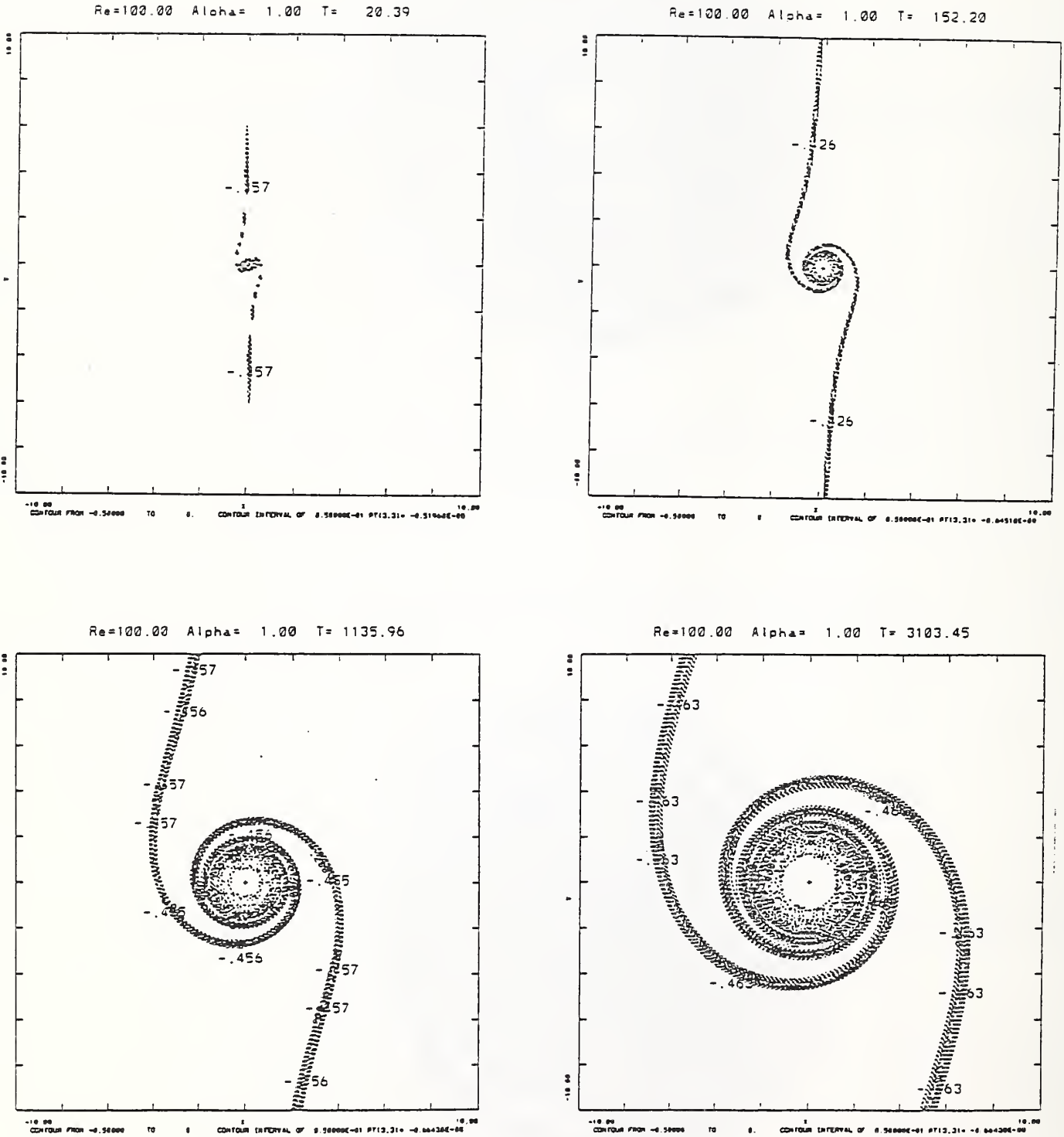
Re=100.00 Alpha= 1.00 T= 20.39
-.457
-.457
Re=100.00 Alpha= 1.00 T= 152.20
-.426
-.426
Re=100.00 Alpha= 1.00 T= 1135.96
-.457
-.456
-.457
-.456
-.457
-.457
-.456
Re=100.00 Alpha= 1.00 T= 3103.45
-.463
-.463
-.463
-.463
-.463
-.463

Figure 6 W

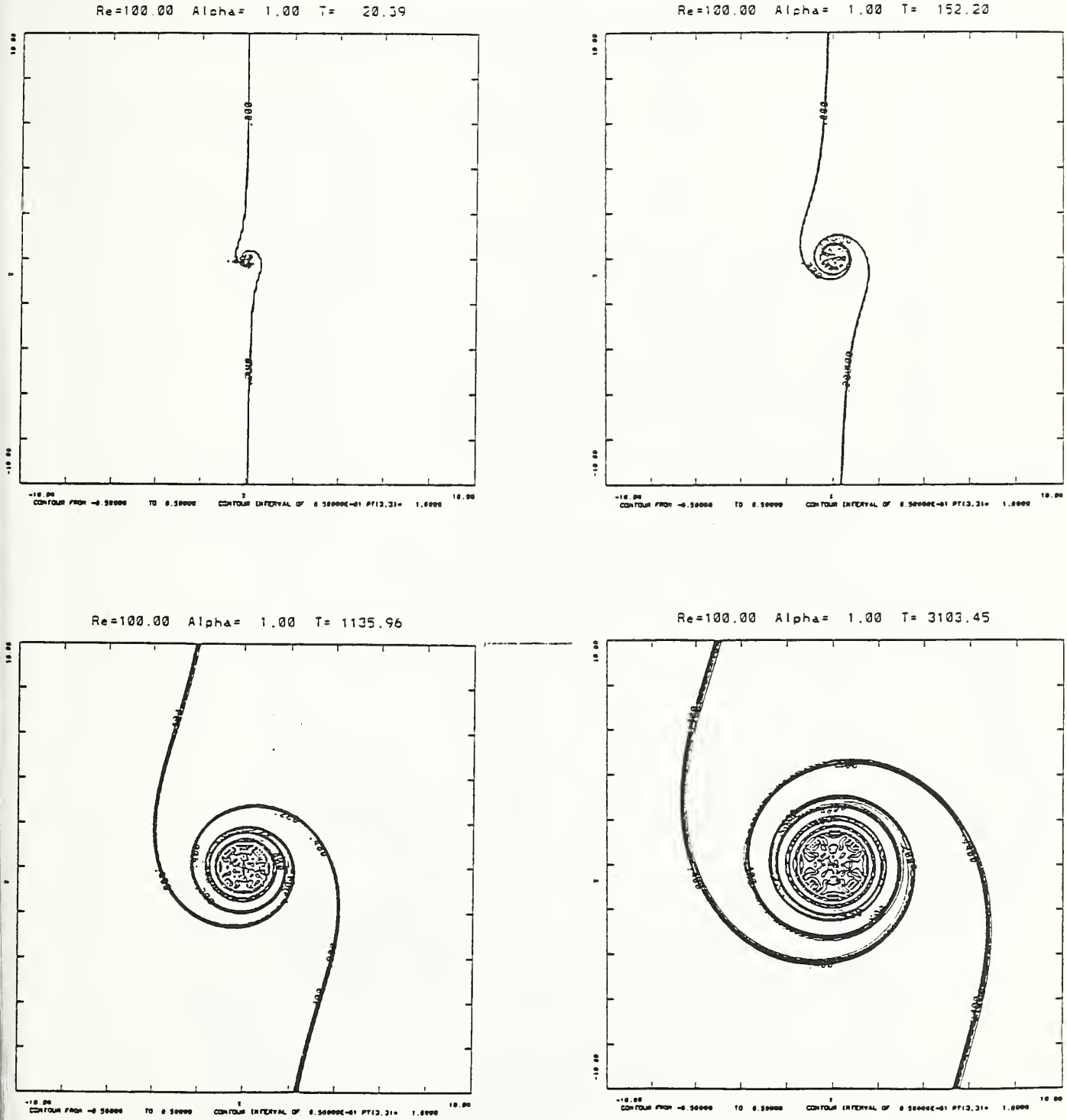
Re=100.00 Alpha= 1.00 T= 20.39
Re=100.00 Alpha= 1.00 T= 152.20
Re=100.00 Alpha= 1.00 T= 1135.96
Re=100.00 Alpha= 1.00 T= 3103.45

Figure 7 *Z*

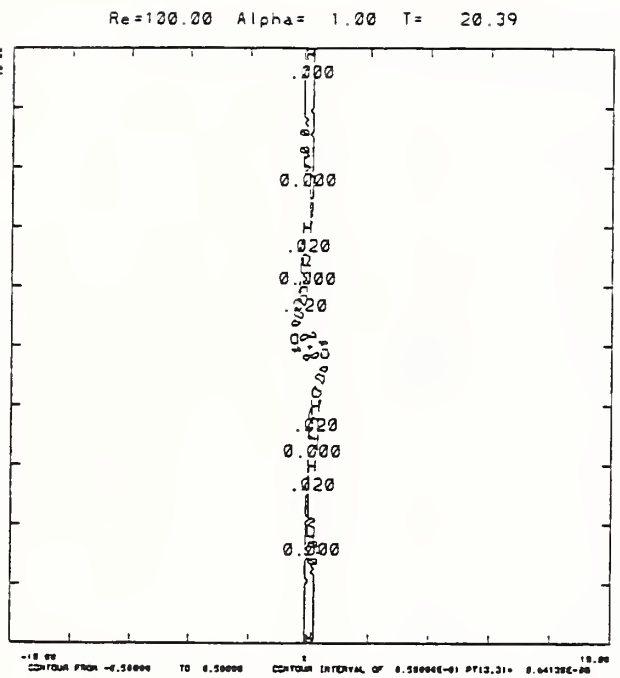

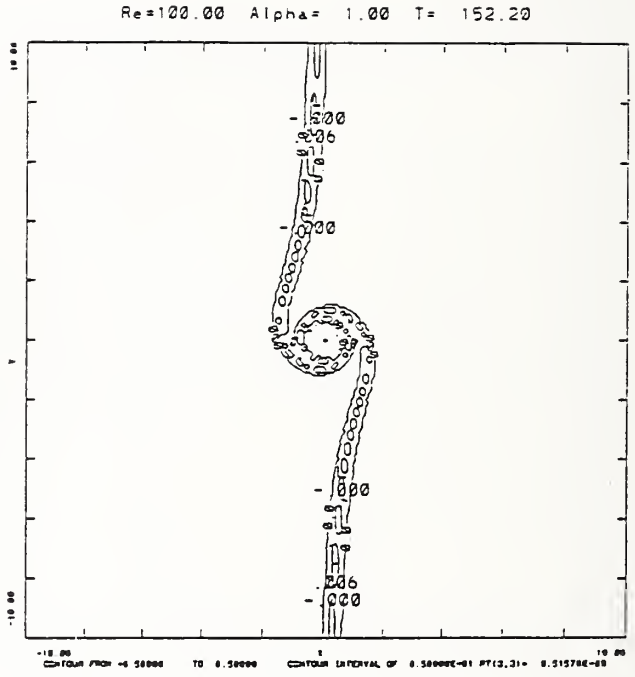

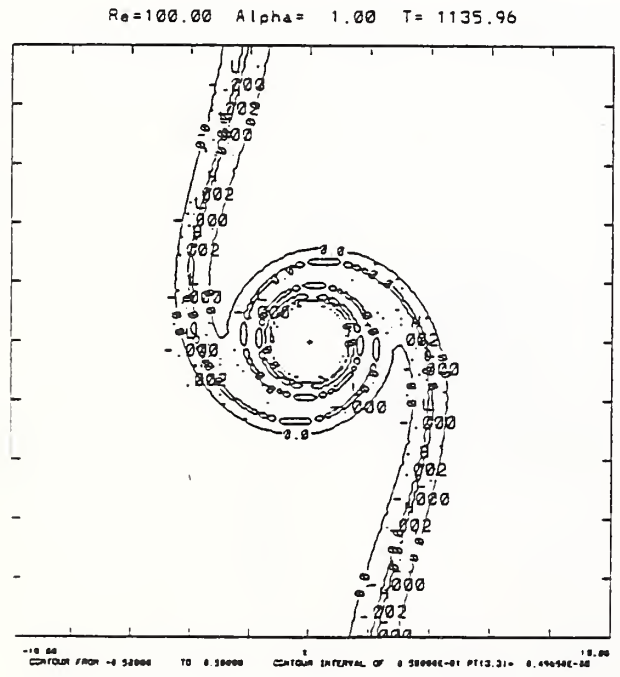

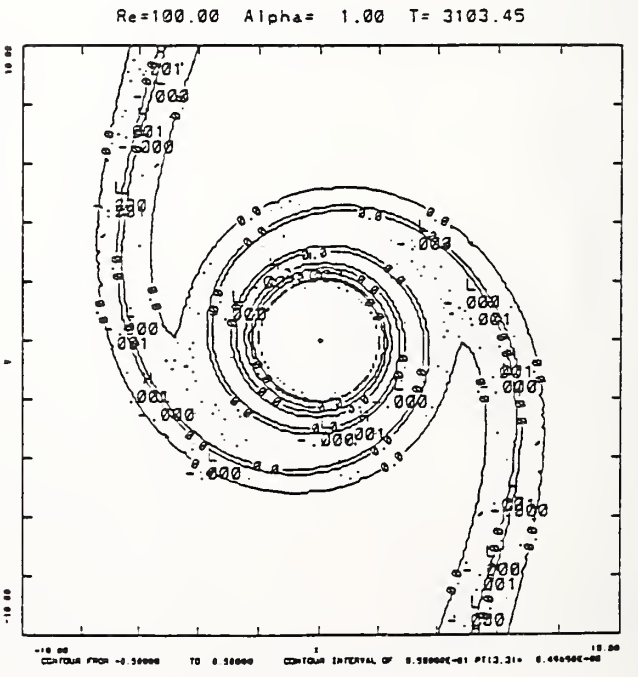

Figure 8 $(W+Z)(\alpha W+1-Z)$

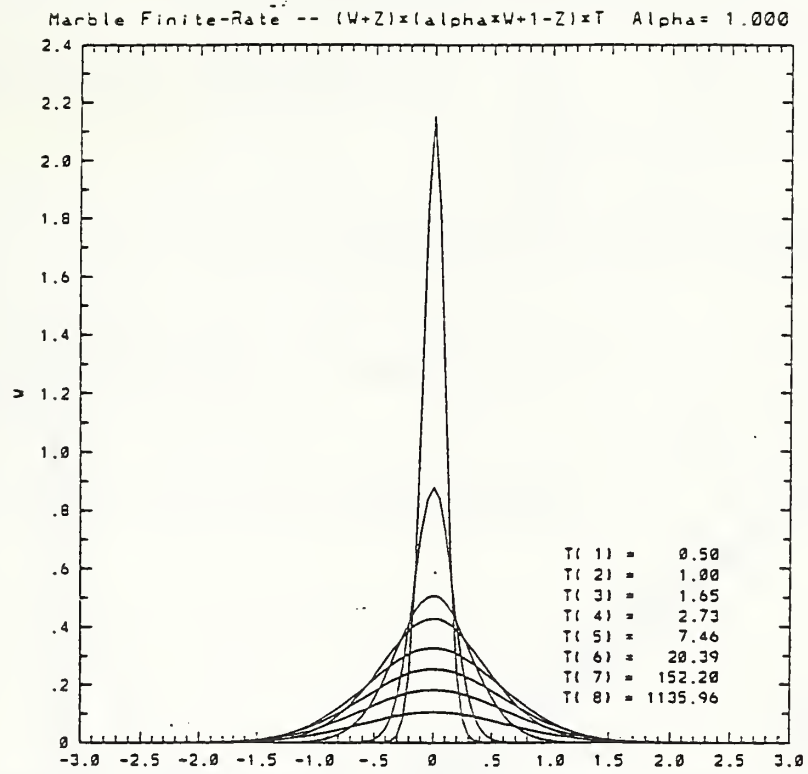

Figure 9a

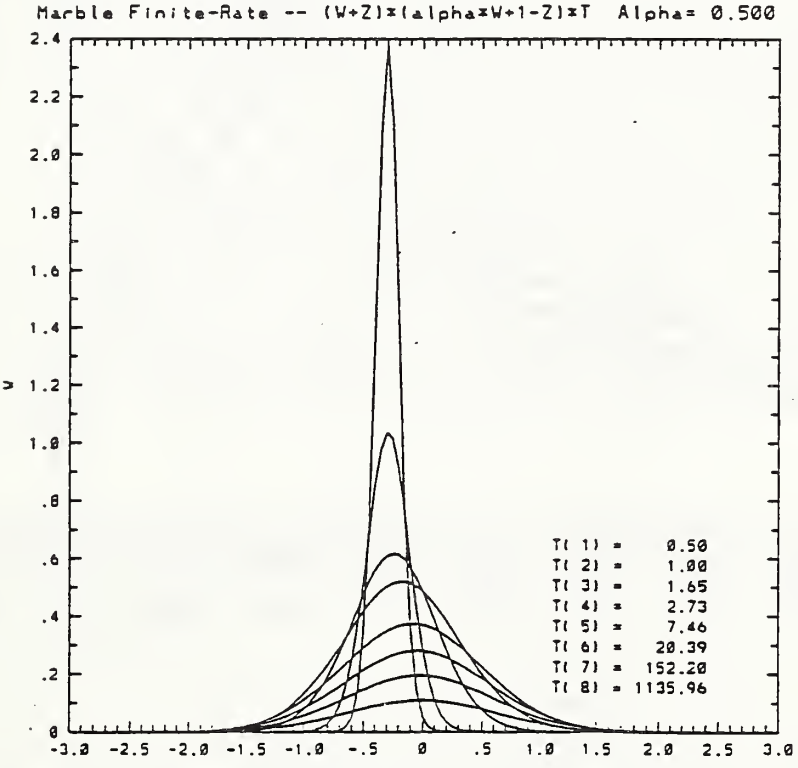

Figure 9b

Figure 10

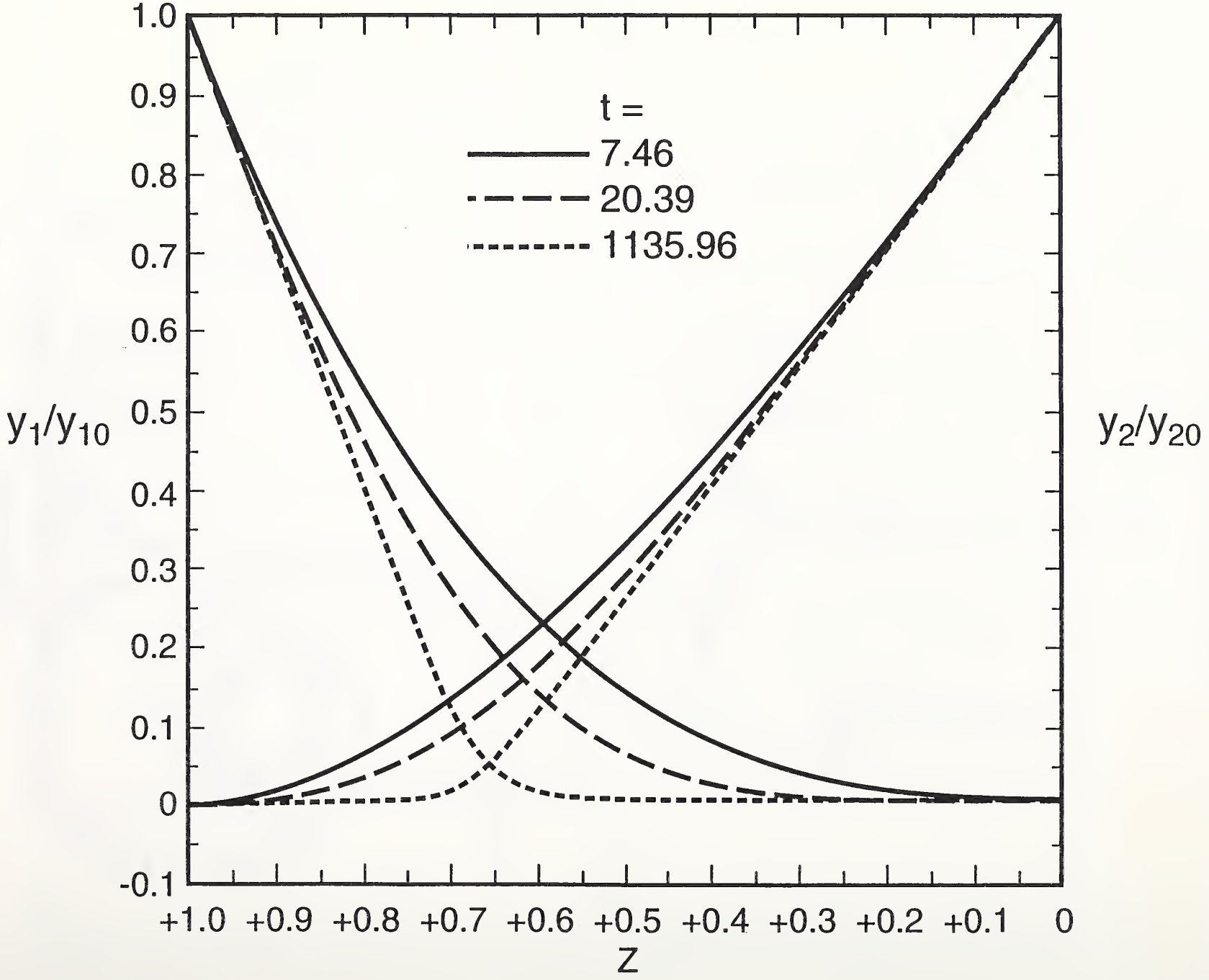
1.0
0.9
0.8
0.7
0.6
0.5
0.4
0.3
0.2
0.1
0
-0.1
t =
7.46
20.39
1135.96
y_1/y_{10}
y_2/y_{20}
+1.0 +0.9 +0.8 +0.7 +0.6 +0.5 +0.4 +0.3 +0.2 +0.1 0
Z

NIST-114A
(REV. 3-90)

U.S. DEPARTMENT OF COMMERCE
NATIONAL INSTITUTE OF STANDARDS AND TECHNOLOGY

BIBLIOGRAPHIC DATA SHEET

1. PUBLICATION OR REPORT NUMBER
NISTIR 4768

2. PERFORMING ORGANIZATION REPORT NUMBER

3. PUBLICATION DATE
February 1992

4. TITLE AND SUBTITLE

Finite-Rate Diffusion-Controlled Reaction in a Vortex, A Report

5. AUTHOR(S)

R.G. Rehm, H.R. Baum, H.C. Tang, and D.W. Lozier

6. PERFORMING ORGANIZATION (IF JOINT OR OTHER THAN NIST, SEE INSTRUCTIONS)

U.S. DEPARTMENT OF COMMERCE
NATIONAL INSTITUTE OF STANDARDS AND TECHNOLOGY
GAITHERSBURG, MD 20899

7. CONTRACT/GRANT NUMBER

8. TYPE OF REPORT AND PERIOD COVERED

9. SPONSORING ORGANIZATION NAME AND COMPLETE ADDRESS (STREET, CITY, STATE, ZIP)

10. SUPPLEMENTARY NOTES

11. ABSTRACT (A 200-WORD OR LESS FACTUAL SUMMARY OF MOST SIGNIFICANT INFORMATION. IF DOCUMENT INCLUDES A SIGNIFICANT BIBLIOGRAPHY OR LITERATURE SURVEY, MENTION IT HERE.)

A two-dimensional model of a constant-density diffusion-controlled reaction with finite reaction-rate chemistry occurring between unmixed species initially occupying adjacent half-spaces is formulated and analyzed. The chemical reaction term is taken to be appropriate for an isothermal, bimolecular reaction for simplicity. An axisymmetric viscous vortex field satisfying the Navier-Stokes equations winds up the interface between the species as they diffuse together and react. The diffusion rates for the two species are assumed contant and equal so that mixture fraction or Shvab-Zeldovich variable can be used. The resulting equation for the mixture fraction is linear and can be solved by noting that a Lagrangian coordinate system removes the convection and that the equation permits a global similarity solution. The single nonlinear equation for one species is also analyzed in a Lagrangian coordinate system. The dimensionless equations depend upon three parameters, Reynolds number, Schmidt number and the initial species concentration ratio, while the dimensionless time plays the role of a Damköhler number. For large Schmidt numbers, a simple expression for the mixture fraction can be obtained and the nonlinear equation for the species concentration can also be substantially simplified. Asymptotic and numerical results show the structure of the reaction region and the competing influences of reaction, diffusion and convection.

12. KEY WORDS (6 TO 12 ENTRIES; ALPHABETICAL ORDER; CAPITALIZE ONLY PROPER NAMES; AND SEPARATE KEY WORDS BY SEMICOLONS)

Analytical; Asymptotics; Combustion; Fires; Nonpremixed combustion; Simulation and Analysis; Turbulent combustion

13. AVAILABILITY

[X] UNLIMITED

[ ] FOR OFFICIAL DISTRIBUTION. DO NOT RELEASE TO NATIONAL TECHNICAL INFORMATION SERVICE (NTIS).

[ ] ORDER FROM SUPERINTENDENT OF DOCUMENTS, U.S. GOVERNMENT PRINTING OFFICE, WASHINGTON, DC 20402.

[X] ORDER FROM NATIONAL TECHNICAL INFORMATION SERVICE (NTIS), SPRINGFIELD, VA 22161.

14. NUMBER OF PRINTED PAGES
31

15. PRICE
A03

ELECTRONIC FORM